ELSEVIER

Marine Geology 247 (2008) 84–103

MARINE GEOLOGY
INTERNATIONAL JOURNAL OF MARINE GEOLOGY, GEOCHEMISTRY AND GEOPHYSICS

www.elsevier.com/locate/margeo

Activity of the turbidite levees of the Celtic–Armorican margin (Bay of Biscay) during the last 30,000 years: Imprints of the last European deglaciation and Heinrich events

S. Toucanne [a,*], S. Zaragosi [a], J.F. Bourillet [b], F. Naughton [a], M. Cremer [a], F. Eynaud [a], B. Dennielou [b]

[a] *Université Bordeaux 1, UMR 5805-EPOC, Avenue des Facultés, F-33405 Talence, France*
[b] *IFREMER, GM/LES, BP70, 29280 Plouzané Cedex, France*

Received 2 February 2007; received in revised form 8 August 2007; accepted 16 August 2007

Abstract

High-resolution sedimentological and micropaleontological studies of several deep-sea cores retrieved from the levees of the Celtic and Armorican turbidite systems (Bay of Biscay — North Atlantic Ocean) allow the detection of the major oscillations of the British–Irish Ice Sheet (BIIS) and 'Fleuve Manche' palaeoriver discharges over the last 30,000 years, which were mainly triggered by climate changes.

Between 30 and 20 cal ka, the turbiditic activity on the Celtic–Armorican margin was weak, contrasting with previous stratigraphic models which predicted a substantial increase of sediment supply during low sea-level stands. This low turbidite deposit frequency was most likely the result of a weak activity of the 'Fleuve Manche' palaeoriver and/or of a reduced seaward transfer of sediments from the shelf to the margin. However, two episodes of turbiditic activity increase were detected in the Celtic–Armorican margin, during Heinrich events (HE) 3 and 2. This strengthening of the turbiditic activity was triggered by the meltwater releases from European ice sheets and glaciers favouring the seaward transfer of subglacial material, at least via 'Fleuve Manche' palaeoriver.

At around 20 cal ka, a significant increase of turbidite deposit frequency occurred as a response to the onset of the last deglaciation. The retreat of the European ice sheets and glaciers induced a substantial increase of the 'Fleuve Manche' palaeoriver discharges and seaward transfer of continentally-derived material into the Armorican turbidite system. The intensification of the turbiditic activity on the Celtic system was directly sustained by the widespread transport of subglacial sediments from the British–Irish Ice Sheet (BIIS) to the Celtic Sea via the Irish Sea Basin. A sudden reduction of turbiditic activity in the Armorican system, between ca. 19 and 18.3 cal ka, could have been triggered by the first well known abrupt sea-level rise ('meltwater pulse', at around 19 cal ka) favouring the trapping of sediment in the 'Fleuve Manche' palaeoriver valleys and the decrease of the seaward transfer of continentally-derived material.

The maximum of turbiditic activity strengthening in the Celtic–Armorican margin, between ca. 18.3 and 17 cal ka, was induced by the decay of European ice sheets and glaciers producing the most extreme episode of the 'Fleuve Manche' palaeoriver runoff and a great seaward transfer of subglacial material into the Bay of Biscay. Between ca. 17.5 and 16 cal ka, the turbiditic activity significantly decreased in both Celtic and Armorican turbidite systems in response to a global re-advance of glaciers and ice sheets in Europe. The last episode of ice sheet retreat, between ca. 16 and 14 cal ka, is well expressed in the Celtic system by a new

* Corresponding author. Tel.: +33 5 40 00 84 38; fax: +33 5 56 84 08 48.
E-mail address: s.toucanne@epoc.u-bordeaux1.fr (S. Toucanne).

0025-3227/$ - see front matter
doi:10.1016/j.margeo.2007.08.006

increase of the turbiditic activity. The major episode of sea-level rise at around 14 cal ka ('Meltwater Pulse 1A'), precluding the seaward transfer of sediments, induced the end of turbiditic activity in both the Celtic and the Armorican system.

Although two main phases of global sea-level rise seem to have had an effect on the Celtic–Armorican margin, this work proposes the BIIS retreat and associated riverine discharges as the main trigger mechanisms of the turbiditic activity in this region during the last 30,000 years.

Keywords: Bay of Biscay; British–Irish Ice Sheet; 'Fleuve Manche'; palaeoriver; last deglaciation; LGM; Heinrich events; turbidites

1. Introduction

It is widely acknowledged that climate change and resulting sea-level oscillations affect in some way the sedimentary processes operating along continental margins and in particular fine-grained turbidite systems (Stow et al., 1985). This is the case of non-glaciated margins located at mid- to low latitudes of the eastern North Atlantic (south of 26°N), far way from glaciers (e.g. Weaver et al., 2000). Inversely, the eastern North Atlantic margin (north of 56°N) and adjacent submarine fans have been particularly affected by ice sheet oscillations during the last part of the full-glacial period (e.g. Dowdeswell et al., 2002; Elverhoi et al., 1998). The effectiveness of ice sheets for sustained glaciated margins is recorded in the Bear Island Fan (western Barents Sea — 75°N). The Bear Island Fan has a similar area and volume to the low-latitude fluvially-derived Amazon and Mississippi turbidite systems but a smallest drainage basin (Dowdeswell et al., 2002) suggesting that the adjacent glaciers have a great ability to erode their substrate. Recent surging glaciers (e.g. Gilbert et al., 2002) also show the close connection between sediment supply and ice sheet oscillations in the high-latitude continental margins.

The Celtic and Armorican turbidite systems (Bay of Biscay — 46°N) are located at the transition zone between the eastern North Atlantic glaciated and non-glaciated margins. Weaver and Benetti (2006) have suggested that deep-sea sedimentation in this region is mostly like influenced by sea-level changes. However, previous studies on continuous hemipelagic sequences suggest that the Celtic–Armorican margin was affected by the British–Irish Ice Sheet (BIIS) oscillations and in particular during an extreme episode of meltwater discharge via the 'Fleuve Manche' palaeoriver at around 18 cal ka (Eynaud et al., 2007; Mojtahid et al., 2005; Zaragosi et al., 2001b). A recent multi-proxy study on three turbidite levees from northern Celtic–Armorican margin also suggests that the BIIS oscillations have had an impact on the deep-sea clastic sedimentation during the last deglaciation and can provide important information about palaeoenvironmental changes at a high-resolution time-scale (Zaragosi et al., 2006).

However, none of these studies have showed how sedimentary processes operating along this continental margin have been affected by the successive BIIS oscillations occurring between the final stages of the last glacial and the last glacial–interglacial transition (LGIT). The aim of this study is therefore to investigate the relationship between gravity processes in the Celtic and Armorican turbidite systems and the BIIS oscillations for the last 30,000 years. Towards this aim we have performed a high-resolution sedimentological and micropaleontological study from five long piston cores (MD04-2836, MD04-2837, MD03-2690, MD03-2688 and MD03-2695) retrieved in turbidite levees of the Celtic–Armorican margin. In particular, we have estimated the frequency of turbidite deposits which allow quantification of the continental sediment supply removing the problems inherent to local sedimentation rate and/or of coring deformations (Skinner and McCave, 2003).

2. Geological and environmental settings

The Celtic–Armorican margin is a passive margin composed of two medium-sized deep-sea clastic systems: the Celtic and the Armorican turbidite systems (Droz et al., 1999; Le Suavé, 2000; Zaragosi et al., 2001a; Zaragosi et al., 2000). The Celtic and Armorican turbidite systems are located in the northern and central part of the Bay of Biscay abyssal plain respectively (Fig. 1), and have been active since the Early Miocene (Droz et al., 1999; Mansor, 2004). Each system covers about 30,000 km^2 in water depths ranging from 4100 m to 4900 m. The turbidite systems are sustained by more than thirty deep canyons capturing continentally-derived sediments. These canyons converge down to five submarine drainage basins (Bourillet et al., 2003) (Fig. 1):

- The 'Grande Sole' extends from the Goban to the Brenot spurs. The Whittard channel–levee system (Fig. 2) is located basinwards of this catchment area;
- The 'Petite Sole' extends from the Brenot to the Berthois spurs and nourishes the Shamrock channel–levee system (Fig. 2);

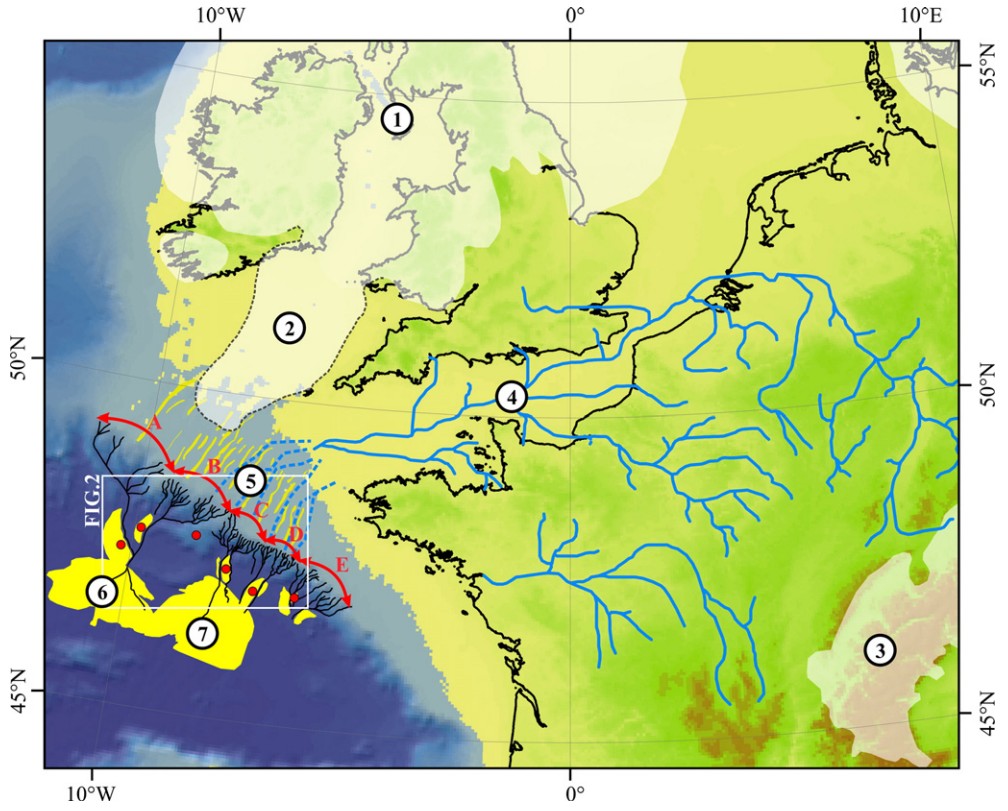

Fig. 1. Physiography of the Celtic–Armorican margin (north-western Europe) during the Last Glacial Maximum (LGM). (1) Extent of the British–Irish Ice Sheet (BIIS) (Bowen et al., 2002); (2) southern extent of the Irish Sea ice stream proposed by Scourse and Furze (2001); (3) extent of the European Alps glacier; (4) 'Fleuve Manche' palaeoriver (Bourillet et al., 2003); (5) Celtic sand banks (Reynaud et al., 1999); fluvial palaeovalleys (blue dashed lines) (Larsonneur et al., 1982); submarine drainage basins: (A) 'Grande Sole', (B) 'Petite Sole', (C) 'la Chapelle', (D) 'Ouest Bretagne', (E) 'Sud Bretagne' (Bourillet et al., 2003); (6) Celtic turbidite system (Droz et al., 1999; Zaragosi et al., 2000); (7) Armorican turbidite system (Zaragosi et al., 2001a). Red circles indicate the core locations. (For interpretation of the references to colour in this figure legend, the reader is referred to the web version of this article.)

- The 'La Chapelle' is located between the Berthois and the Delesse spurs and connects the Blackmud and Guilcher channel–levee systems;
- The 'Ouest Bretagne' is located between the Delesse and the Bourcart spurs linking downstream with the Crozon channel–levee system;
- The 'Sud Bretagne', located between the Bourcart and the Folin spurs, is linked downstream to the Audierne channel–levee system (Fig. 2).

During the last glacial period, the Celtic and Armorican turbidite systems seems to have been particularly influenced by the British–Irish Ice Sheet (BIIS) oscillations and 'Fleuve Manche' palaeoriver discharges (e.g. Bourillet et al., 2003). It is widely known that the 'Fleuve Manche' palaeoriver activity started during the last glacial period, favoured by the lowering of the sea-level stand and by episodes of the BIIS meltwater discharge (Mojtahid et al., 2005; Zaragosi et al., 2001b) which covered Great Britain and Ireland during the last glacial period (e.g. Bowen et al., 2002). The 'Fleuve Manche' palaeoriver had a large catchment area, including the continental palaeodrainage system of major West European palaeorivers such as the Rhine, Meuse, Seine, Somme, Thames and Solent (Bourillet et al., 2003; Lericolais, 1997) (Fig. 1).

Besides the 'Fleuve Manche' palaeoriver, the Irish Sea Basin seems to have played an important role in sediment supply from the continent to the Celtic–Armorican margin. It is known that the Irish Sea ice stream protruded in the southern Irish Sea and Celtic Sea although its extent is still a matter of debate. Recent simulations (Boulton and Hagdorn, 2006) and geological field studies (Evans and O'Cofaigh, 2003; Hiemstra et al., 2006; O'Cofaigh and Evans, 2007) seem to confirm that the southern limit of this ice stream reached the Isles of Scilly, as previously suggested by Scourse (1991) and Scourse et al. (1990) (Fig. 1).

Many studies from marine deep-sea cores have showed that the BIIS was very sensitive to abrupt climatic changes (e.g. Knutz et al., 2007; Peck et al., 2006) and in particular

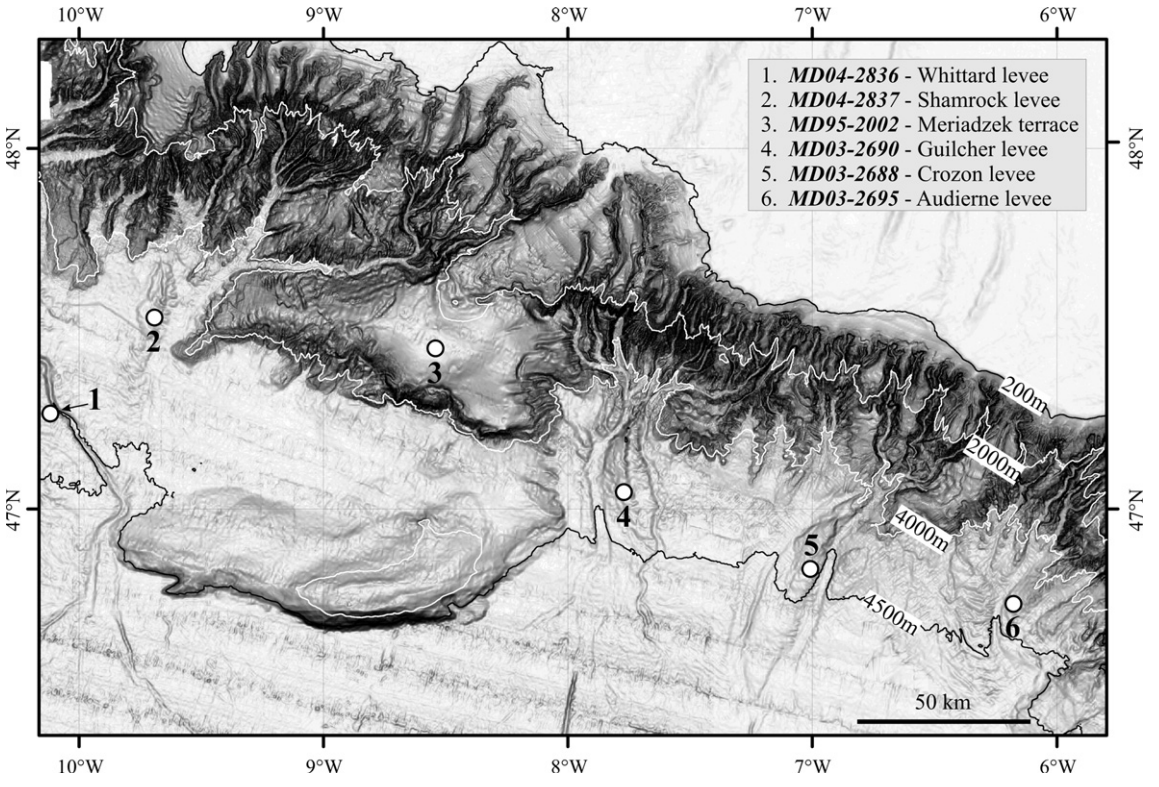

Fig. 2. Shaded morphologic map of the Celtic–Armorican margin. White circles and associated numbers indicate core locations.

during the last deglaciation (Eynaud et al., 2007; Mojtahid et al., 2005; Zaragosi et al., 2006; Zaragosi et al., 2001b). This hypothesis has been confirmed by several continental studies which reveal a progressive but complex decay of the BIIS during the last deglaciation (McCabe and Clark, 1998; McCabe et al., 2007b).

3. Materials and methods

Five long piston cores (Table 1) were retrieved by using the 'Calypso' corer in the Celtic–Armorican margin during the MD133-SEDICAR (Bourillet and Turon, 2003) and the MD141-ALIENOR (Turon and Bourillet, 2004) oceanographic cruises on board the *R/V Marion Dufresne* (IPEV). Cores MD03-2688, MD03-2690 and MD03-2695 were recovered in the Crozon, Guilcher and Audierne turbidite levees (Armorican turbidite system) while cores MD04-2836 and MD04-2837 were collected in the Whittard and Shamrock turbiditic levees (Celtic turbidite system) (Fig. 1 and 2). Previous studies on this region have shown that some of these turbidite levees are mainly composed of a complex sedimentological

Table 1
Key parameters of cores discussed in this study including core number, geographic position, water depth and oceanographic missions

Core number	Latitude	Longitude	Depth (m)	Cruise	Year	Institute
MD95-2002	47° 27.12′ N	08° 32.03′ W	2.174	MD105-IMAGE 1	1995	IFREMER
MD03-2688	46° 48.03′ N	07° 02.93′ W	4.385	MD133-SEDICAR	2003	IFREMER
MD03-2690	47° 01.25′ N	07° 44.99′ W	4.340	MD133-SEDICAR	2003	IFREMER
MD03-2695	47° 43,14′ N	06° 12,68′ W	4.375	MD133-SEDICAR	2003	IFREMER
MD04-2836	47° 16.57′ N	10° 07.69′ W	4.362	MD141-ALIENOR	2004	IFREMER
MD04-2837	47° 31.99′ N	09° 44.01' W	4.176	MD141-ALIENOR	2004	IFREMER

Table 2
Radiocarbon ages of cores MD04-2836, MD03-2688, MD03-2690 and MD03-2695 and of the neighbouring core MD95-2002

Core number	Depth (cm)	Material	Laboratory number	Corrected ^{14}C age (yr BP)	Calendar age (cal yr BP)	Data origin
MD95-2002	0	*G. Bulloides*	LSCE-99360	1660+/−70	1624	Zaragosi et al. (2001a,b)
MD95-2002	140	*G. Bulloides*	LSCE-99361	9080+/−90	10,329	Zaragosi et al. (2001a,b)
MD95-2002	240	*N. pachyderma* s.	LSCE-99362	10,790+/−100	12,809	Zaragosi et al. (2001a,b)
MD95-2002	420	*N. pachyderma* s.	LSCE-99363	13,330+/−130	15,798	Zaragosi et al. (2001a,b)
MD95-2002	454	*N. pachyderma* s.	LSCE-99364	13,800+/−110	16,426	Zaragosi et al. (2001a,b)
MD95-2002	463	*N. pachyderma* s.	LSCE-99365	14,020+/−120	16,709	Zaragosi et al. (2001a,b)
MD95-2002	510	*N. pachyderma* s.	LSCE-99366	14,170+/−130	16,897	Zaragosi et al. (2001a,b)
MD95-2002	550	*N. pachyderma* s.	SacA-003242	14,430+/−70	17,327	Zaragosi et al. (2006)
MD95-2002	580	*N. pachyderma* s.	Beta-141702	14,410+/−200	17,332	Zaragosi et al. (2001a,b)
MD95-2002	869	*N. pachyderma* s.	SacA-003243	14,900+/−70	18,241	Zaragosi et al. (2006)
MD95-2002	875	*N. pachyderma* s.	SacA-003244	14,880+/−160	18,224	Zaragosi et al. (2006)
MD95-2002	1320	*G. Bulloides*	SacA-003245	18,450+/−90	22,062	Zaragosi et al. (2006)
MD95-2002	1340	*G. Bulloides*	SacA-003246	19,030+/−100	22,514	Zaragosi et al. (2006)
MD95-2002	1390	*G. Bulloides*	SacA-003247	20,220+/−80	24,690	Zaragosi et al. (2006)
MD95-2002	1424	*N. pachyderma* s.	Beta-123696	19,840+/−60	23,777	Grousset et al. (2000)
MD95-2002	1453	*N. pachyderma* s.	Beta-123698	20,030+/−80	23,984	Grousset et al. (2000)
MD95-2002	1464	*N. pachyderma* s.	Beta-123699	20,200+/−80	24,174	Grousset et al. (2000)
MD95-2002	1534	*N. pachyderma* s.	Beta-123697	21,850+/−70	25,734	Grousset et al. (2000)
MD95-2002	1610	*N. pachyderma* s.	Beta-99367	24,010+/−250	28,222	Auffret et al. (2002)
MD95-2002	1664	*N. pachyderma* s.	Beta-99368	25,420+/−230	29,830	Auffret et al. (2002)
MD04-2836	100.5			9275	10,700	Correlation MD95-2002
MD04-2836	150.5	*N. pachyderma* s.	SacA-003248	10,730+/−50	12,788	Zaragosi et al. (2006)
MD04-2836	411.5			11,900	13,938	Correlation MD95-2002
MD04-2836	1354.5	*N. pachyderma* s.	SacA-003249	12,840+/−120	15,159	Zaragosi et al. (2006)
MD04-2836	1656.5	*N. pachyderma* s.	SacA-003253	13,480+/−60	16,017	Zaragosi et al. (2006)
MD04-2836	1761.5	*N. pachyderma* s.	SacA-003254	14,210+/−70	16,956	Zaragosi et al. (2006)
MD04-2836	2131,5	*N. pachyderma* s.	SacA-005971	14,650+/−50	17,727	This paper
MD04-2836	2534.5			15,091	18,396	Correlation MD95-2002
MD04-2836	3525.5	*N. pachyderma* s.	SacA-003256	17,090+/−80	20,209	Zaragosi et al. (2006)
MD03-2688	157	*G. bulloides*	SacA-004927	8495+/−35	9541	This paper
MD03-2688	480	*N. pachyderma* s.	SacA-004928	12,580+/−90	14,751	This paper
MD03-2688	1084	*N. pachyderma* s.	SacA-004929	14,200+/−70	16,941	This paper
MD03-2688	1704	*N. pachyderma* s.	SacA-004930	14,650+/−110	17,699	This paper
MD03-2688	1955			15,091	18,396	Correlation MD95-2002
MD03-2688	2422	*G. bulloides*	SacA-004931	16,930+/−80	20,057	This paper
MD03-2688	2695			20,220	23,722	Correlation MD95-2002
MD03-2688	2910	*N. pachyderma* s.	SacA-004932	21,570+/−110	25,410	This paper
MD03-2688	3136	*N. pachyderma* s.	SacA-004933	24,890+/−140	29,227	This paper
MD03-2688	3520	*G. bulloides*	SacA-004793	29,160+/−180	34,038	This paper
MD03-2690	151	*G. Bulloides*	SacA-001894	8730+/−60	9900	Zaragosi et al. (2006)
MD03-2690	245	*G. Bulloides*	SacA-003233	9450+/−60	10,774	Zaragosi et al. (2006)
MD03-2690	425			11,900	13,938	Correlation MD95-2002
MD03-2690	626	*G. Bulloides*	SacA-003234	12,620+/−60	14,863	Zaragosi et al. (2006)
MD03-2690	692	*N. pachyderma* s.	SacA-003235	12,770+/−70	15,074	Zaragosi et al. (2006)
MD03-2690	1094	*N. pachyderma* s.	SacA-003236	13,840+/−70	16,483	Zaragosi et al. (2006)
MD03-2690	1213	*N. pachyderma* s.	SacA-003237	14,030+/−70	16,715	Zaragosi et al. (2006)
MD03-2690	1885	*N. pachyderma* s.	SacA-003238	14,650+/−70	17,717	Zaragosi et al. (2006)
MD03-2690	2233	*N. pachyderma* s.	SacA-003239	14,960+/−70	18,287	Zaragosi et al. (2006)
MD03-2690	2276	*N. pachyderma* s.	Poz. Rad. Lab.	15,080+/−70	18,392	Zaragosi et al. (2006)
MD03-2690	2923	*G. Bulloides*	SacA-005972	16,990+/−110	20,115	This paper
MD03-2690	3156	*G. Bulloides*	SacA-003240	18,850+/−100	22,378	Zaragosi et al. (2006)
MD03-2690	3376	*N. pachyderma* s.	SacA-003241	20,560+/−70	24,600	Zaragosi et al. (2006)
MD03-2690	3576	*N. pachyderma* s.	Poz. Rad. Lab.	21,880+/−120	25,769	Zaragosi et al. (2006)
MD03-2695	242			13,463	15,970	Correlation MD95-2002
MD03-2695	878	*N. pachyderma* s.	SacA-005609	14,640+/−60	17,703	This paper
MD03-2695	1187.5	*N. pachyderma* s.	SacA-005610	14,830+/−60	18,030	This paper

Table 2 (*continued*)

Core number	Depth (cm)	Material	Laboratory number	Corrected ^{14}C age (yr BP)	Calendar age (cal yr BP)	Data origin
MD03-2695	1347	*N. pachyderma* s.	SacA-005611	14,990+/−60	18,305	This paper
MD03-2695	1420			15,091	18,396	Correlation MD95-2002
MD03-2695	1991	*N. pachyderma* s.	SacA-005612	17,130+/−70	20,248	This paper
MD03-2695	2255	*N. pachyderma* s.	SacA-005613	20,300+/−100	24,284	This paper
MD03-2695	2393			22,028.2	26,032	Correlation MD95-2002
MD03-2695	2444	*N. pachyderma* s.	SacA-005614	25,600+/−150	30,034.4	This paper
MD03-2695	2600			27,400	32,068	Elliot et al., 2001 (HE3)
MD03-2695	2758	*N. pachyderma* s.	SacA-005616	28,710+/−210	33,536.2	This paper

Radiocarbon ages of this study were performed at the 'Laboratoire de Mesure du Carbone 14' in Saclay ('SacA'). Radiocarbon dates have been corrected for a marine reservoir effect of 400 years and calibrated to calendar years using CALIB Rev 5.0/Marine04 data set (Hughen et al., 2004; Stuiver and Reimer, 1993; Stuiver et al., 2005) up to 21.78 ^{14}C ka and Bard et al. (1998) thereafter.

succession of turbiditic sequences alternating with ice-rafted laminae and hemipelagic layers (Zaragosi et al., 2006).

3.1. Chronostratigraphy

The age models for cores MD03-2688, MD03-2690, MD03-2695 and MD04-2836 have been determined based on foraminiferal stratigraphy, AMS dating and by using additional control points from the reference core MD95-2002 (Table 2). The age model of core MD95-2002 was based on 20 ^{14}C AMS ages spanning the last 30 ka (Table 2) (Auffret et al., 2002; Grousset et al., 2000; Zaragosi et al., 2006; Zaragosi et al., 2001b).

Cores were sub-sampled with a sample spacing of 5 to 20 cm for micropaleontological analysis along the hemipalegic layers. These hemipelagic layers are not contaminated by reworked material and represent intervals of continuous sedimentation. The subsamples were then dried, weighed and washed through a 150 μm mesh sieve. At least 300 polar foraminifera *Neogloboquadrina pachyderma* (s.) were counted jointly with a number of other planktonic species in order to determine the relative abundances (%) of this polar species. Previous studies on this region have shown the suitable use of *N. pachyderma* (s.) to reconstruct drastic sea surface changes which are stratigraphically contemporaneous with major climatic events (Mojtahid et al., 2005; Peck et al., 2007; Zaragosi et al., 2001b).

Thirty four accelerator mass spectrometer (AMS) ^{14}C dates were obtained from cores MD03-2688, MD03-2690, MD03-2695 and MD04-2836 (Table 2).

3.2. Sedimentological analyses

The sedimentological analyses of the Celtic–Armorican deep-sea cores consist firstly of visual description and X-ray analysis obtained with a SCOPIX image processing tool (Migeon et al., 1999). Additionally, grain-size analysis were performed using a Malvern™ Supersizer 'S'. Finally, microscopical observations of about ten thin-sections (10 cm long) of impregnated sediments selected from well-preserved and representative sedimentary facies were performed using a fully automated Leica™ DM6000B Digital Microscope. The last method has been recently detailed in Zaragosi et al. (2006).

In order to understand the activity of the Celtic and Armorican turbidite systems, we have detected and quantified the number of turbiditic deposits in the Whittard, Guilcher, Crozon and Audierne turbidite levees. For this, we firstly observed several thin-sections of impregnated sediments representing distinctive alternated facies of ice-rafted, turbiditic deposits and hemipelagic layers (Fig. 3). Secondly, we have determined the criteria to distinguish each facies via microscope and X-ray imagery. Finally, we applied these criteria to distinguish each facies in all cores using X-ray imagery. Indeed, microscopic observation of IRD laminae reveals heterogeneous and scattered angular lithic grains within fine-bioturbated clay while fine (mm-thick) and slightly dark layers are observed in the X-ray imagery (Fig. 3). Turbiditic deposits are generally thicker (mm-thick to cm-thick) than IRD laminae and present usually sharply eroded basal contacts. The progressive transition from very dense (dark) contacts to a slightly lighter (grey) top of sequences, visible on X-ray imagery, is associated with the typical fining-up trend of turbiditic deposits (Bouma, 1962; Stow and Piper, 1984) (Fig. 3).

Each turbiditic deposit of cores MD04-2836, MD03-2690, MD03-2688 and MD03-2695 has been counted using X-ray imagery. Turbidites have not been counted in core MD04-2837 because this record presents important disturbances linked to coring stretching. Following this, we have quantified the turbidite deposit frequency on the Whittard, Guilcher, Crozon and Audierne levees per

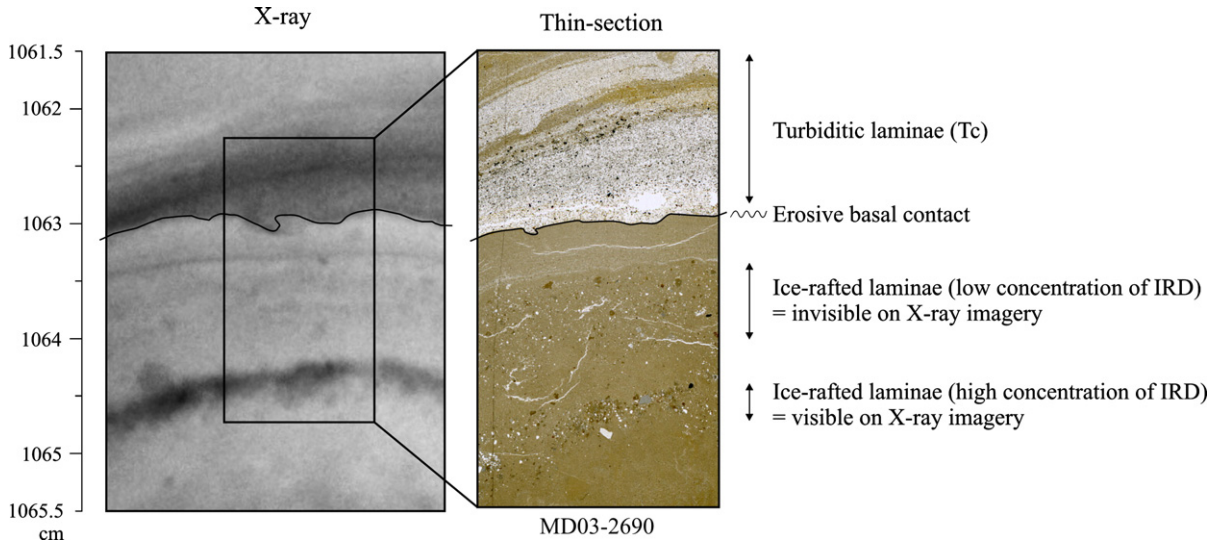

Fig. 3. Recognition of turbiditic and ice-rafted laminae on X-ray imagery and on the microscope using thin-sections of impregnated sediment.

1000 years. We assumed that this quantification represents the minimum value of turbidite frequency because of possible erosive losses and/or non-deposit events (i.e. by-pass).

4. Results

4.1. Chronological framework

It is usually difficult to reconstruct an accurate stratigraphy in turbidite levees because these environments are mainly composed of reworked sedimentary material. Therefore, we have used the abundance peaks of *N. pachyderma* (s.) determined in well-preserved hemipelagic material as primary tool to establish the age model of cores MD04-2836, MD04-2837, MD03-2688, MD03-2690 and MD03-2695. This method allows the detection of several paleoclimatic events during the end of the Marine Isotopic Stages (MIS) 3, MIS 2 and MIS 1: Heinrich events (HE 3, HE 2 and HE 1), Last Glacial Maximum (LGM), Greenland Interstadial 1 (GIS1)/ Bölling–Alleröd (BA), Younger Dryas (YD) and the Holocene (Fig. 4).

The maximum expansion of the polar foraminifera *N. pachyderma* (s.) in the Celtic–Armorican margin between ca. 18.3 and 16 cal ka (Fig. 4), suggesting extremely cold sea surface waters, is contemporaneous with the presence of ice-rafted detritus (IRD) in the reference core MD95-2002 (Zaragosi et al., 2001b). Although IRD are detected between ca. 18.3 and 16 cal ka, their maximum expression occurred within the interval 17–16 cal ka. The age limits of this cold episode are synchronous with those proposed by Elliot et al. (2001) for Heinrich (HE) 1 event elsewhere in the North Atlantic region. The other episodes of *N. pachyderma* (s.) maximum expansion (~90–100%) occurring at ca. 23.5–26 cal ka and at ca. 30–32 cal ka are also synchronous with the age limits of HE 2 and HE 3, respectively (Elliot et al., 2001). We assume therefore that these cooling events detected in the Celtic–Armorican margin are most likely the result of the impact of Heinrich events. Previous works on the eastern North Atlantic (e.g. Bond et al., 1992; Eynaud et al., 2007) have shown a sea surface cooling episode preceding the maximal arrival of IRD. Other records from the mid-latitudes of the North Atlantic region have shown the same complex pattern in both marine and terrestrial environments, which have been associated to the well known Heinrich events (e.g. Bard et al., 2000; Chapman et al., 2000; Naughton et al., 2007; Naughton et al., submitted for publication).

The Younger Dryas cold period is also defined by the increase of the *N. pachyderma* (s.). However, an intriguing sedimentary hiatus is observed at around this period in cores MD03-2688 and MD03-2695 (Fig. 4). The planktonic foraminiferal assemblages show that the Early Holocene and Bølling–Allerød periods are well recorded in both cores (Duprat, *comm. pers.*).

Furthermore, radiocarbon results have confirmed that core-to-core correlations, based on abrupt increases in abundances of *N. pachyderma* (s.), represent the temporal limits of the cold episodes that punctuated the final part of the last glacial period (Table 2 and Fig. 4).

The age model of core MD03-2688 indicates that this core covers the last ca. 34 cal ka (~29.1 ^{14}C ka); core MD03-2695 extends back to ca. 33.5 cal ka (~28.7 ^{14}C ka)

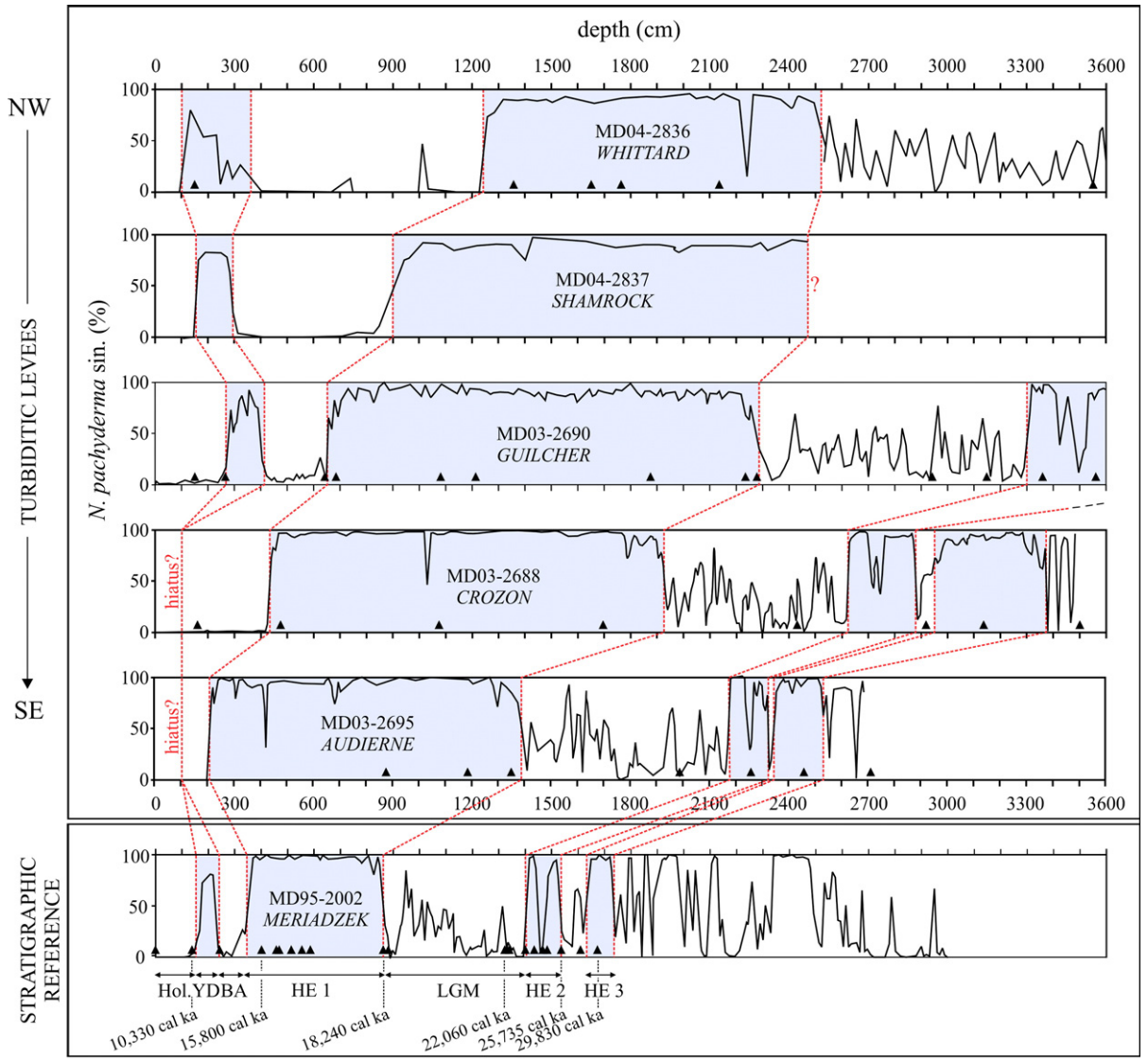

Fig. 4. Abundance (%) of foraminifera *N. pachyderma* (s.) in cores MD04-2836, MD04-2837, MD03-2690 (Zaragosi et al., 2006), MD03-2688, MD03-2695 (this study) and MD95-2002 (Zaragosi et al., 2001b). Black triangles indicate the depth of samples used for AMS dating. Blue shading corresponds to cold periods. Dashed red lines represent core-to-core correlation using the limits of cold episodes. Hol: Holocene, YD: Younger Dryas, BA: Bölling–Alleröd, HE: Heinrich events (1 to 3), LGM: Last Glacial Maximum. (For interpretation of the references to colour in this figure legend, the reader is referred to the web version of this article.)

and core MD03-2690 to ca. 26 cal ka (~22 ^{14}C ka); and core MD04-2836 spans ca. 20.4 cal ka (~17.3 ^{14}C ka) (Fig. 4 and Table 2).

4.2. Evolution of sedimentary conditions

The detailed sedimentological analysis (visual description, X-ray imagery, grain-size measurements and thin-section analysis) of the studied cores has allowed the identification of six lithofacies (Figs. 5, 7 and 8). These lithofacies represent the evolution of the sedimentary conditions on the Whittard, Blackmud, Guilcher, Crozon and Audierne levees during the last 30,000 years (Fig. 5):

Lithofacies 1, between 0 and 8 cal ka (Mid- and Late-Holocene), is constituted by homogeneous, structureless marly ooze containing a temperate foraminiferal assemblage (*Globigerinoides ruber*, *Globigerina bulloides*, *Globorotalia hirsuta*, *Globorotalia truncatulinoides*, *Orbulina universa*) (Fig. 5). This lithofacies forming the modern deep-sea Bay of Biscay seafloor has been interpreted on the turbidite levees as a pelagic to hemipelagic drape deposits without significant turbidite

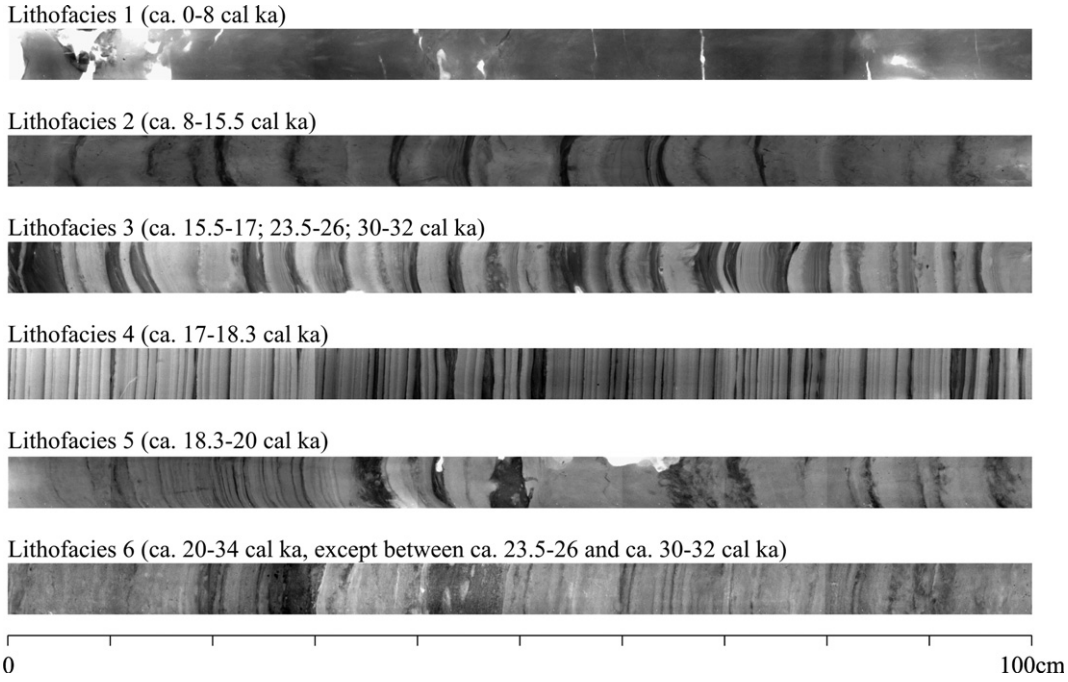

Fig. 5. Examples of some representative X-rayed slabs of lithofacies 1 to 6.

supplies from the continental shelf (Zaragosi et al., 2006).

Lithofacies 2, between ca. 8 and 15.5 cal ka, consists of homogeneous structureless clay interbedded with some centimetre-scale silt to very fine sand layers (Fig. 5). Sedimentation rates range from 270 to 370 cm ka^{-1} and reach 770 cm ka^{-1} in core MD04-2836 (Fig. 6). Beds display a sharply erosive basal contact and are normally graded, with a basal grain-size median ranging from 20 to 80 μm in core MD04-2836, 40 to 80 μm in core MD03-2690 and 60 to 140 μm in core MD03-2688. According to Stow and Piper (1984), these beds represent silt-mud turbidites deposited from the overflow of turbidity currents while homogeneous clay is interpreted as hemipelagic deposits.

Lithofacies 3, between ca. 15.5 and 17 cal ka, ca. 23.5 and 26 cal ka and ca. 30.5 and 32 cal ka., shows a monospecifism of the polar foraminifera *N. pachyderma* (s.) and contains frequent thinning- and fining-upward sequences of very fine sand and silt deposits with erosive basal contacts (Fig. 5). These sequences are interpreted as fine-grained turbidites. Turbidite layers are thin (1 to 10 cm) and their basal grain-size ranges from 40 to160 μm in core MD04-2836, 50 to 140 μm in core MD03-2690, 30 to110 μm in core MD03-2688 and 15 to 100 μm in core MD03-2695. Numerous IRD-rich millimetre-scale clay layers are also interbedded with the turbidite sequences. Sedimentation rates range from 110 to 500 cm ka^{-1} in cores MD04-2836 and MD03-2690 respectively (Fig. 6). Lithozone 3 reveals periods of important turbidite deposits associated with numerous ice-rafting events on the sedimentary levees of the Celtic–Armorican margin.

Lithofacies 4, between ca. 17 and 18.3 cal ka, is an ultra-laminated sediment composed of IRD-rich millimetre-scale clay layers and fine fining-upward silty laminae with sharp basal contacts (Figs. 5 and 7). Some silty to very fine sandy deposits are also observed and show thin cross-rippled laminations. These laminations are interpreted to be of turbiditic origin. Their basal grain-size ranges from 40 to 140 μm in cores MD04-2836 and MD03-2690, 20 to 120 μm in core MD03-2688 and 20 to 180 μm in core MD03-2695. Load casts and flame structures are commonly present at the lower contacts of the turbidites. A monospecifism of *N. pachyderma* (s.) is also described in lithofacies 4. Sedimentation rates are extremely high (>600 cm ka^{-1}) and reach up to 950 cm ka^{-1} in core MD03-2695 (Fig. 6). Lithofacies 4 reveals a high sediment supply period produced by very frequent turbidity currents in the channel–levee systems and numerous ice-rafting events.

Lithofacies 5, between ca. 18.3 cal ka and ca. 20 cal ka, is characterized by homogeneous structureless clay interbedded with some fining-upward millimetre- to centimetre-scale silt to sand deposits with erosive basal

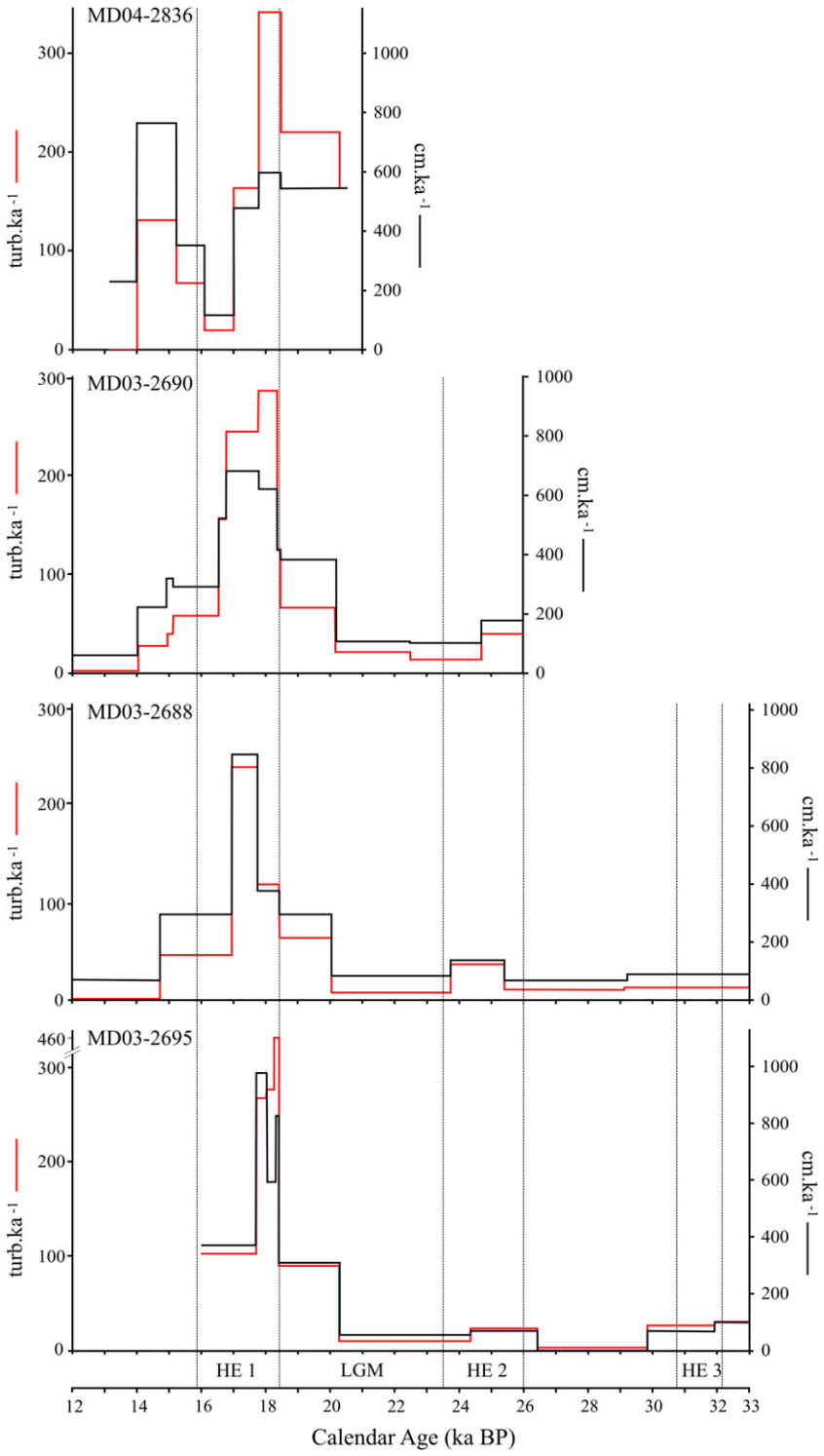

Fig. 6. Evolution of sedimentation rates (continuous black line — cm ka^{-1}) and of turbidite deposit frequency (continuous red line — turb ka^{-1}) in cores MD04-2836, MD03-2690, MD03-2688 and MD03-2695. Although sedimentation rates must be considered with precaution because of frequent oversampling in Calypso piston cores (Skinner and McCave, 2003), the resulting curves parallel those of the turbidite deposit frequency suggesting that sedimentation rates can be considered as fairly valid. (For interpretation of the references to colour in this figure legend, the reader is referred to the web version of this article.)

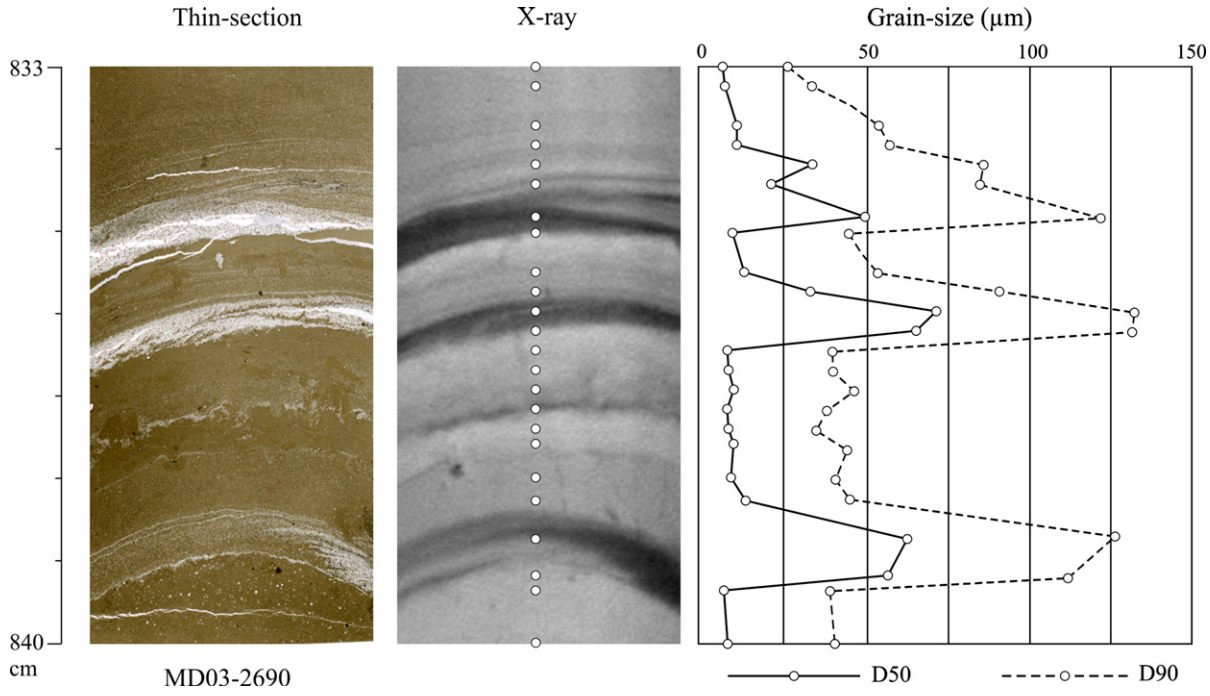

Fig. 7. Example of a thin-section of impregnated sediment (left) from lithofacies 4 in core MD03-2690, X-ray (middle) and grain-size measurements (right). D50 (continuous line) = grain-size at which 50% of sample is finer; D90 (dashed line) = grain-size at which 90% of sample is finer. Open circles represent the chosen samples used for grain-size analysis. Black layers represent turbidite deposits in the X-ray imagery.

contacts (Fig. 5). These sequences are interpreted as fine-grained turbidites. Some parts of the top of lithofacies 5 are laminated and represent a transition zone between the ultra-laminated lithofacies 4 and the base of the lithofacies 5 which is mostly composed of scattered centimetre-scale turbidites. The grain-size of the base of turbidite beds ranges from 40 to 160 μm in core MD04-2836, 50 to 190 μm in core MD03-2690, 60 to 240 μm in core MD03-2688 and 50 to 230 μm in core MD03-2695. Mean sedimentation rates range from 290 to 375 cm ka^{-1} except in core MD04-2836 where it reaches 545 cm ka^{-1} (Fig. 6). Lithofacies 5 shows hemipelagic sedimentation interbedded with some turbidites deposits that are more massive and more spaced in its basal part, thus defining a transition sedimentary facies between lithofacies 4 and lithofacies 6.

Lithofacies 6 was deposited between ca. 20 and 34 cal ka, except during ca. 23.5–26 cal ka and ca. 30.5–32 cal ka periods which corresponds to lithofacies 3. Lithozone 6 is dominated by massive, fining-upward silt to sand deposits, interpreted as turbidites (Figs. 5 and 8). Grain-size appears to be similar to that characterising lithofacies 5. However, turbidites of lithofacies 6 are thicker (centimetre to decimetre-scale) than turbidites of lithofacies 5. Sedimentation rates are moderate to low with values ranging from 15 to 100 cm ka^{-1} (Fig. 6). Lithofacies 6 reveals a period of rare but massive turbidity current activity.

4.3. Turbidite deposit frequency

The frequency of the turbiditic deposits (turb ka^{-1}) has been estimated from cores MD04-2836, MD03-2690, MD03-2688 and MD03-2695 for the last 30 ka (Figs. 6, 9 10 and 11). Three main periods of turbiditic activity are observed:

a) From ca. 33 to 20 cal ka, there is a general low turiditic activity in the Guilcher, Crozon and Audierne channel–levee systems. The turbidite deposit frequency ranges from 0 to 40 turbidites per thousand years (turb ka^{-1}). A moderate frequency of turbiditic deposits occurred during HE 3 and HE 2 (30 to 40 turb ka^{-1}) while low turbiditic activity (max. 15 turb ka^{-1}) is associated with the end of MIS 3 and the early- and mid-LGM (Figs. 6 and 9).
b) Between ca. 20 to 17 cal ka, there is a general huge increase in the frequency of the turbidite deposits (75 turb ka^{-1} in core MD03-2688 and 230 turb ka^{-1} in core MD04-2836) (Figs. 6, 9 and 10). A higher resolution study of the frequency of the turbidite deposits (number of turbidites per 250 years), in core

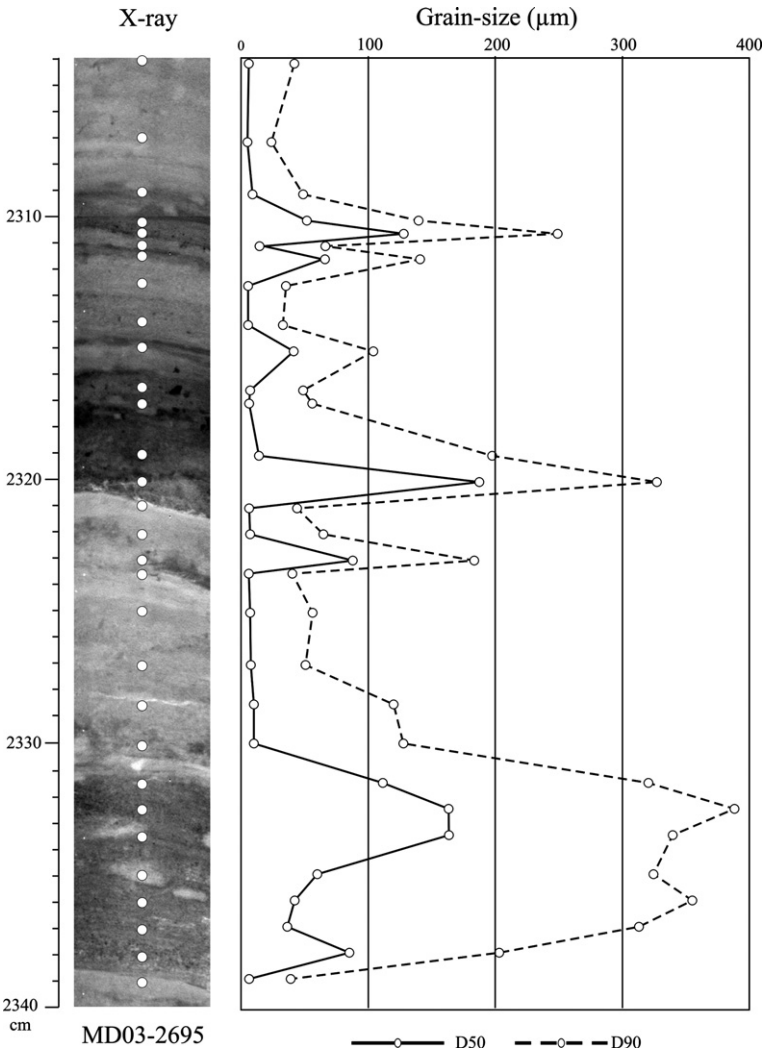

Fig. 8. Example of an X-rayed slab (left) from lithofacies 6 in core MD03-2695 and grain-size measurements (right). D50 (continuous line) = grain-size at which 50% of sample is finer; D90 (dashed line) = grain-size at which 90% of sample is finer. Open circles represent the chosen samples used for grain-size analysis. Black layers represent turbidite deposits in the X-ray imagery.

MD03-2688, shows a sudden episode of turbidite deposit frequency decrease between ca. 19 and 18.3 cal ka (Fig. 10). The turbiditic activity reached a maximum intensity between ca. 18.3 to 17 cal ka in all cores independently of the time resolution used to calculate those frequencies (Figs. 6, 9 and 10).

c) From ca. 17 to 16 cal ka, there is a sharp decrease of the turbiditic activity in all cores. The turbidite deposit frequency reached 60 to 120 turb ka^{-1} on the Guilcher, Crozon and Audierne levees and only 25 turb ka^{-1} on the Whittard levee between 17 and 16 cal ka (Figs. 6, 9, 10 and 11).

d) From ca. 16 to 0 cal ka, although there is a gradual decrease of the turbiditic activity in most areas (Figs. 6, 9, 10 and 11), Whittard records shows a significant reactivation of gravity processes at the beginning of this interval. Indeed, turbidite deposit frequency of core MD04-2836 reaches 130 turb ka^{-1} between ca. 16 and 14 cal ka while attaining only 25 turb ka^{-1} between ca. 17–16 cal ka and 8 turb ka^{-1} between ca. 14–13 cal ka (Fig. 11).

5. Discussion

5.1. Implications of the BIIS and 'Fleuve Manche' palaeoriver activities in the Celtic–Armorican margin during the last 30 ka

The high-resolution sedimentological and micropaleontological study of several marine deep-sea cores

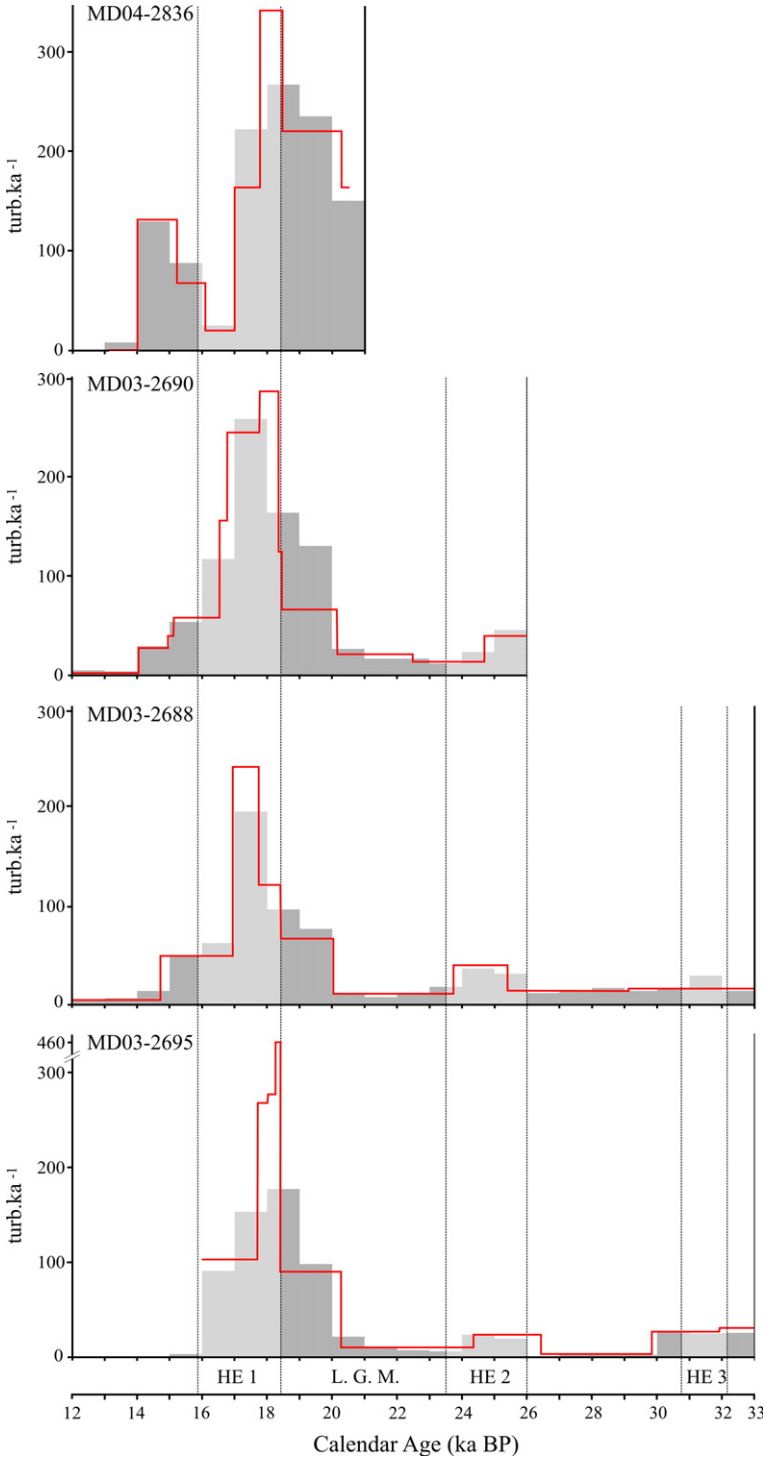

Fig. 9. Evolution of the turbidite deposit frequency (histograms — turb ka^{-1}) using time slices (1 ka) of the age models of cores MD04-2836, MD03-2690, MD03-2688 and MD03-2695. The continuous red line represents the frequency of turbidite deposits (turb ka^{-1}) calculated by using two consecutive control points. (For interpretation of the references to colour in this figure legend, the reader is referred to the web version of this article.)

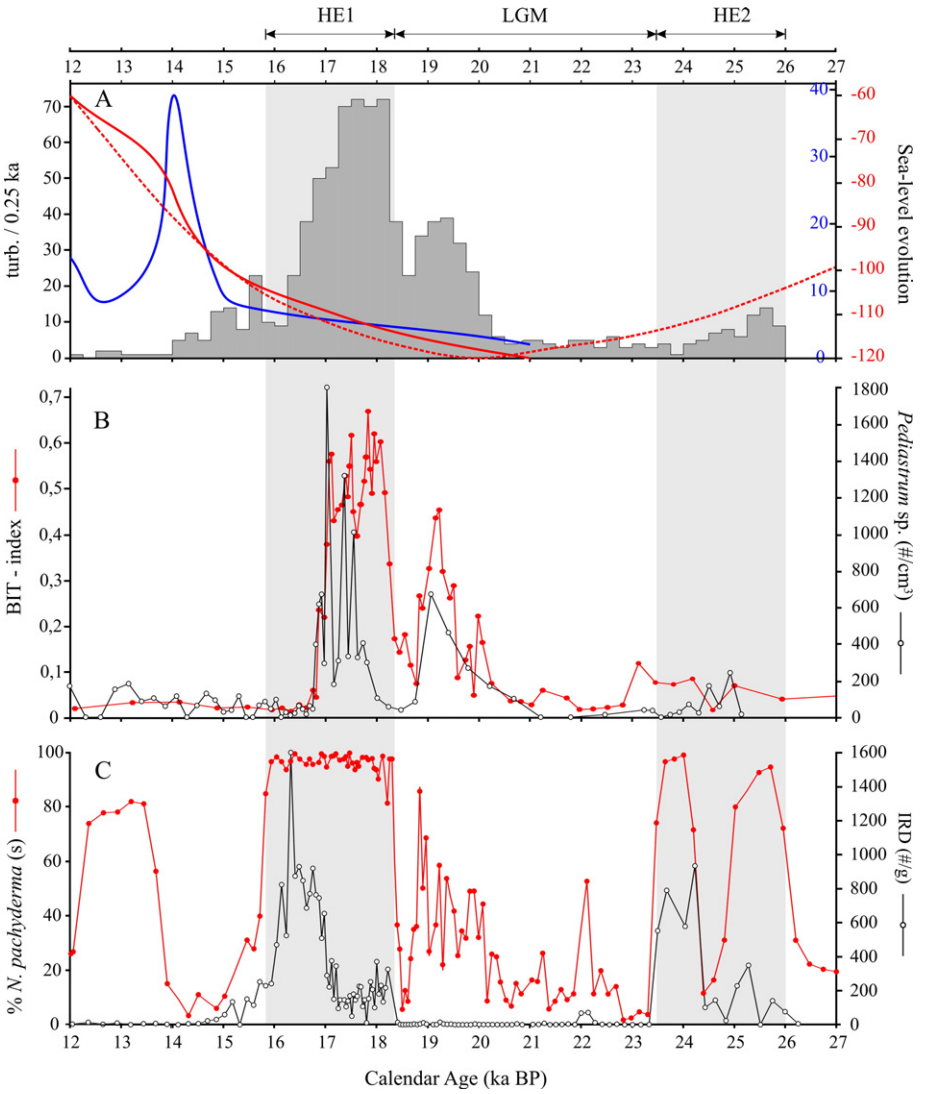

Fig. 10. Comparison between: (A) sedimentologic data of core MD03-2690 and (B, C) palaeoclimatic records of core MD95-2002 between 27 and 12 cal ka. (A) Histogram represents the turbidite deposit frequency with a 250-year resolution (turb./0.25 ka). Red curves show the relative sea-level evolution (m) described by Fairbanks (1989) (continuous line) and by Waelbroeck et al. (2002) (dashed line). Blue line represents the rate of sea-level rise (mm a^{-1}) and the 'Meltwater Pulse 1A' (MWP 1A — ca. 14 cal ka) (Fairbanks, 1989). (B) BIT-index (Ménot et al., 2006) and *Pediastrum* sp. abundances (# cm^{-3}) (Eynaud, 1999; Zaragosi et al., 2001b). (C) Abundances of IRD > 150 μm (# g^{-1}) and *N. pachyderma* (s.) (%) (Zaragosi et al., 2001b). (For interpretation of the references to colour in this figure legend, the reader is referred to the web version of this article.)

retrieved on the turbidite levees of the Whittard, Blackmud, Guilcher, Crozon and Audierne channel–levee systems allows the detection of the major BIIS oscillations and 'Fleuve Manche' palaeoriver discharges during the last 30 ka. The turbidite deposit frequency estimated in MD04-2836, MD03-2690, MD03-2688 and MD03-2695 deep-sea cores reflects important oscillations of sediments supply into the Celtic and Armorican turbidite systems between 30 ka and 14 ka BP (Figs. 6 and 9).

The last glacial period is marked by the long-term increase of the global ice volume, contemporaneous with the global sea-level fall (Chappell, 2002; Lambeck et al., 2002). The last sea-level lowstand, contemporaneous with the final stages of the global ice expansion occurred between ca. 30 and ca. 20 cal ka (Lambeck et al., 2002). However, during this interval, several millennial-scale climate oscillations have been observed in both Greenland and North Atlantic records (Bond et al., 1993; Dansgaard et al., 1993) producing substantial sea-level changes (Siddall et al., 2003). In this work, we define the LGM as a period of relatively stable climate that occurred between HE 2 and HE 1 following

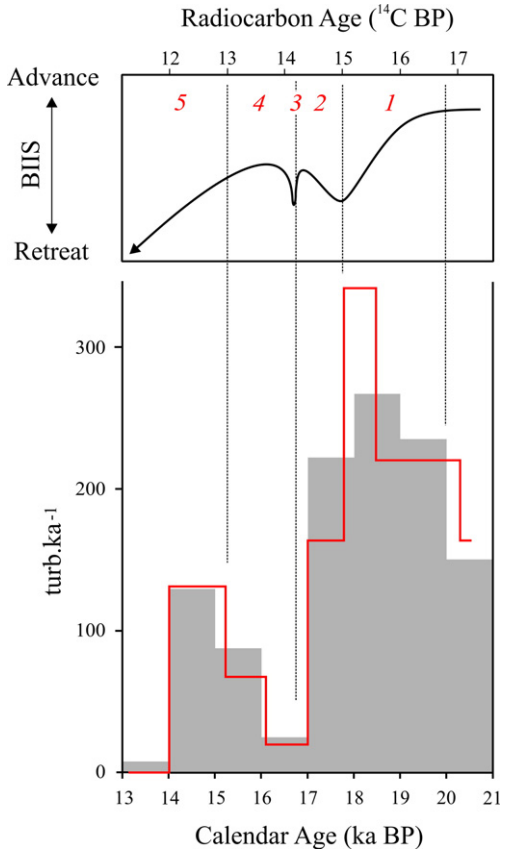

Fig. 11. Comparison between turbidite deposit frequency in the Celtic turbidite system (core MD04-2836) (this study) and the BIIS oscillations in the Irish Sea Basin (McCabe et al., 2007b). Continuous red line show the frequency of turbidite deposits (turb ka^{-1}) between two consecutive control points of the age model of core MD04-2836 while the histogram show the turbidite deposit frequency using a time slicing of 1 ka. 1: 'Cooley Point Interstadial' (from ≥16.7 to ≤15 ^{14}C ka BP); 2: 'Clogher Head Stadial' (from ≥15 to ≤14.2 ^{14}C ka BP); 3: 'Linns Interstadial' (~14.2 ^{14}C ka BP); 4: 'Killard Point Stadial' (from ≥14.2 to ~13.0 ^{14}C ka BP); 5: 'Rough Island Interstadial' (after ~13.0 ^{14}C ka BP) (McCabe et al., 2007b). Note the close relationship between the main retreat periods of the BIIS and enhanced turbiditic activity in the Whittard channel. (For interpretation of the references to colour in this figure legend, the reader is referred to the web version of this article.)

the EPILOG (Mix et al., 2001) and MARGO (Kucera et al., 2005) suggestions.

It is commonly accepted that sea-level lowstand conditions favoured the seaward sediment transfer from the continent to the deep-sea turbidite systems (e.g. Posamentier and Vail, 1988). Therefore, we should expect to detect a maximum of the turbidite frequency in the Celtic and Armorican turbidite systems synchronous with the last lowest sea-level stand. Our data shows, on the contrary, that there is a general weak sediment supply to the Celtic and Armorican turbidite systems between ca. 30 and ca. 20 cal ka (Figs. 6 and 9). The low turbidite deposit frequency within ca. 30 and 20 cal ka in the Celtic–Armorican margin can probably be due to weak runoff rates of the 'Fleuve Manche' palaeoriver and/or to low seaward sediment transfer which was probably blocked on the shelf as a response to the deposition of sand banks in the Celtic sea (Reynaud et al., 1999). Nonetheless, the presence of some turbidite sequences in this region is most likely the result of sediment seaward transfer from the delta located in the 'Fleuve Manche' palaeoriver mouth (Lericolais, 1997; Zaragosi et al., 2001a). Two episodes of turbidite frequency increase contemporaneous with HE 3 and HE 2 punctuated the general low turbidite activity period (Figs. 6, 9 and 10). This increase of turbiditic activity during HE 3 and HE 2 was likely the result of an increase of seaward transfer of subglacial sediment as a response to meltwater releases from surrounded ice sheets and glaciers, confirming what has been previously proposed by climate simulations (e.g. Clarke et al., 1999; Forsström and Greve, 2004) as well as by sedimentological studies on the eastern Canadian margin (e.g. Hesse et al., 2004; Rashid et al., 2003).

A significant increase of sediment supply shown by the increase of the turbidite deposit frequency is observed since ca. 20 cal ka in cores MD04-2836 (i.e. in the Celtic turbidite system), MD03-2690, MD03-2688 and MD03-2695 (i.e. in the Armorican turbidite system) (Figs. 6 and 9). The quantity of sediment supply into the Celtic turbidite system is higher than that of the Armorican turbidite system.

The 'Grande Sole' drainage basin was connected to the Celtic Sea (Fig. 1) funnelling substantial volume of sediment directly released by the BIIS and the Irish Sea ice stream (Bowen et al., 1986; Eyles and McCabe, 1989) into the Celtic turbidite system via the Irish Sea Basin. The 'Cooley Point Interstadial', starting at ca. 20 cal ka (~16.7 ^{14}C ka BP (McCabe and Clark, 1998)), characterises the beginning of the BIIS deglaciation and induced the widespread transport of subglacial sediments to the south-east Irish ice-margin as previously suggested by several continental records (Bowen et al., 2002; McCabe et al., 2005). The high turbiditic activity in the Whittard channel synchronous with the major episode of the Irish Sea ice stream retreat (Fig. 11) suggests that the Irish Sea Basin was probably affected by fully marine conditions, favouring the direct seaward transfer of sediments from the BIIS. These fully marine conditions were attained because the isostatic depression of the Irish Sea Basin vastly exceeded the eustatic lowering as suggested by Clark et al. (2004) and McCabe et al. (2007a; 2007b).

Although the turbidite deposit frequency in the Armorican turbidite system is lower than that recorded in the Celtic system, an increase of the turbiditic activity has been also detected in cores MD03-2690, MD03-2688 and MD03-2695 at around 20 cal ka (Figs. 6, 9 and 10). This increase of the turbidite deposit frequency in the Armorican turbidite system suggests the strengthening of the 'Fleuve Manche' palaeoriver discharges at around 20 cal ka. Seismic records from this region show the presence of Neogene fluvial palaeovalleys in the present-day shelf (Fig. 1), between the 'Fleuve Manche' palaeoriver and canyons of the Armorican margin (Bourillet et al., 2003). This suggests that these sub-environments were directly connected in the past, favouring the great seaward transfer of sediments from the 'Fleuve Manche' palaeoriver via the numerous canyons which composed the 'La Chapelle', 'Ouest Bretagne' and 'Sud Bretagne' drainage basins (Figs. 1 and 2). Furthermore, previous studies on this region detected an increase of *Pediastrum* sp. concentration (freshwater alga) (Zaragosi et al., 2001b) and of BIT-index (Branched and Isoprenoid Tetraether) (Ménot et al., 2006) reflecting the introduction of high quantities of fluvial terrestrial organic material in the Armorican margin contemporaneous with the increase of turbiditic activity in this area (Fig. 10). Additionally, recent simulations have shown that tides and tidal currents of the Celtic–Armorican shelf also contributed to the seaward transfer of continental material between 20 and 10 ka (Uehara et al., 2006).

The strengthening of the 'Fleuve Manche' palaeoriver discharges was probably induced by the retreat of the BIIS, the European glaciers and the south-western part of the Fennoscandian ice sheet. The well known episodes of glacier decay in Scandinavia (Rinterknecht et al., 2006), Poland (Marks, 2002) and in the European Alps (Hinderer, 2001; Ivy-Ochs et al., 2004) at around ca. 20 cal ka corroborate our hypothesis.

The retreat and melting of the European ice sheets and glaciers at ca. 20 cal ka contributed to an abrupt sea-level rise, known as a 'meltwater pulse' at around 19 cal ka (19-ka MWP) (Clark et al., 2004; Yokoyama et al., 2000). This abrupt episode lasted 500 years and sea-level rise amounted to over 15 m (Yokoyama et al., 2000) favouring the trapping of sediments in the 'Fleuve Manche' palaeoriver valleys. Synchronously, the decrease of both BIT-index and *Pediastrum* sp. concentration in the neighbouring core (MD95-2002) (Ménot et al., 2006; Zaragosi et al., 2001b) (Fig. 10) suggests a decrease of continentally-derived material to the Armorican margin, also supporting the idea of reduced 'Fleuve Manche' discharges in the northern part of the Bay of Biscay.

Following this, the observed abrupt increase of sediment supply in the Celtic and Armorican turbidite systems at ca. 18.3 cal ka (Figs. 6, 9, 10 and 11) was most likely the result of a seaward sediment transfer increase from the south-east Irish ice-margin and an intensification of the 'Fleuve Manche' palaeoriver runoff, respectively. In the Armorican turbidite system, the highest turbidite deposit frequency is synchronous with the maximal arrival of continental material as demonstrated by BIT-index (Ménot et al., 2006) and *Pediastrum* sp. concentration (Zaragosi et al., 2001b) (Fig. 10). This suggests that the 'Fleuve Manche' discharges increased drastically at around 18.3 cal ka confirming what has been previously proposed by Zaragosi et al. (2001b) and Ménot et al. (2006). This episode of high riverine discharges, occurring at ca. 18.3 cal ka, was clearly more intense than that characterizing the beginning of the deglaciation (ca. 20 cal ka) (Figs. 6, 9 and 10) and was also likely the result of the European glacier retreat. Several studies have shown that important environmental changes leading to a substantial retreat of the BIIS occurred in the north and north-western UK margin (Knutz et al., 2002a; Knutz et al., 2002b; Wilson et al., 2002), contemporaneous with the maximum decay of the Fennoscandian ice sheet at ca. 18.3 cal ka (Dahlgren and Vorren, 2003; Lekens et al., 2005; Nygard et al., 2004). The deposition of one ultra-laminated facies in the Celtic–Armorican margin between ca. 18.3 cal ka and 17 cal ka (lithofacies 4 — Fig. 5) reveals that a significant environmental change has had an impact in northern and southern part of the glacially-influenced European margin. This facies has been recognized as marine 'varves' resulting from episodic cycles between meltwater discharges and iceberg calving (Zaragosi et al., 2006).

Between ca. 17.5 and 16 cal ka, there was a decrease of the turbiditic activity in the Celtic turbidite system (Figs. 6, 9 and 11) which was contemporaneous with the two main general re-advance phases of the BIIS: the 'Clogher Head' and 'Killard Point' stadials (after 15 and until ~13 ^{14}C ka BP), detected in the northern Irish Sea Basin by McCabe et al. (2007b). This suggests that subglacial material transfer from the BIIS to the 'Grande Sole' drainage basin was most likely reduced during re-advance episodes of the BIIS. Theses episodes were synchronous with the re-advance of the Fennoscandian ice sheet and central European glaciers (Alps, Jura) (Buoncristiani and Campy, 2004; Everest et al., 2006; Ivy-Ochs et al., 2006; Knies et al., 2007). The rapid decrease of the turbidite deposit frequency in the Armorican turbidite system (Figs. 6, 9 and 10) reveals a substantial decrease of the 'Fleuve Manche'

palaeoriver runoff, in response to the episodic 'pause' of the last deglaciation.

The resumption of the last deglaciation is particularly well expressed in the Celtic turbidite system record during the well known Bölling–Alleröd episode. Indeed, the last major decay of the BIIS, associated with the 'Stagnation Zone Retreat' and the 'Rough Island Interstadial' episodes detected in the northern Irish Sea Basin (McCabe et al., 2005; McCabe et al., 2007b), induced a relatively huge increase of the turbiditic activity in the Celtic turbidite system, between ca. 16 and 14 cal ka (Fig. 11). Besides the last stages of the BIIS decay, the Celtic–Armorican margin was also affected by a rapid and sustained rise of the global sea-level from 16 to 12.5 cal ka (Lambeck et al., 2002). Indeed, the cessation of turbiditic activity on the Celtic–Armorican margin occurred during or after the episode of maximum sea-level rise (Fig. 10), known as the 'Meltwater Pulse 1A' (MWP 1A — ca. 14 cal ka) (Fairbanks, 1989) contributing to the disappearance of the 'Fleuve Manche' palaeoriver. Moreover, the increase of dry conditions in Europe during the Younger Dryas at around 13 cal ka (e.g. Watts, 1980) also decreased the seaward transfer of fluvially-derived sediment onto the Celtic–Armorican margin.

The comparison of the turbiditic activity between the Celtic turbidite system and the Laurentian Fan, which extends at the outlet of the Laurentide Ice Sheet (LIS) (Skene and Piper, 2003), reveals a similar sedimentary pattern over the last deglaciation. Two main phases of turbidite deposition occurred at the end of the LGM and after ca.16 cal ka, bracketing a huge reduction of sediment supply at around 16.5 cal ka. Despite a short time lag between the BIIS and the LIS oscillations over the last deglaciation (McCabe and Clark, 1998), the similarity of both turbiditic records from the Laurentian Fan and the Celtic system suggests that seaward transfer of glacially-derived material to the deep-sea North Atlantic have been clearly forced by the combined effect of global climate changes and amphi-North Atlantic ice sheets oscillations for at least the last 20,000 years.

6. Conclusions

The high-resolution sedimentological (including turbidite frequency analysis) and micropaleontological studies performed in the Celtic–Armorican margin document the evolution of the turbidite systems in this region over the last 30,000 years. Changes in the frequency of turbidite deposits in the Celtic–Armorican margin were mainly triggered by the British–Irish Ice Sheet (BIIS) and European glaciers oscillations (advance and retreat episodes). The retreat of the BIIS and European glaciers favoured the transfer of continentally-derived material via the Irish Sea ice stream and the 'Fleuve Manche' palaeoriver into the Celtic and the Armorican systems respectively. Inversely, the BIIS and European glaciers advances preclude the introduction of large amounts of meltwater into the 'Fleuve Manche' palaeoriver, reducing drastically the seaward transfer of sediments in the Bay of Biscay. This evidence, contrasting with stratigraphic models which predict that turbidite systems are mainly controlled by sea-level changes, confirms that glacially-influenced turbidite systems are largely controlled by ice sheets and glaciers oscillations. However, the synchronicity between turbidite deposit frequency reduction and the abrupt meltwater pulse episode (19-ka MWP) suggests that this drastic sea-level rise would have favoured the trapping of sediments in the 'Fleuve Manche' palaeoriver. Similarly, after the last stage of the BIIS decay a second sudden episode of sea-level rise (MWP 1A) contributed to the end of the 'Fleuve Manche' palaeoriver discharges and consequent turbiditic activity in the Celtic–Armorican margin.

Acknowledgements

The authors warmly thank G. Chabaud, G. Floch, R. Kerbrat, B. Martin, M. Rovere, J. Saint Paul and O. Ther for their technical support and J. Duprat and A. Van Toer for their useful assistance to the biostratigraphic approach. We thank also G. Ménot for data of the BIT-index; P. De Deckker, M. Gaudin and M.F. Sánchez Goñi for valuable comments and language improvement; and the crew and scientific teams of MD133/SEDICAR and MD141/ALIENOR cruises on the '*R/V Marion Dufresne*' (IPEV) for the recovery of the long piston cores. We acknowledge financial support by the French Programme 'GDR MARGES' and 'RELIEFS DE LA TERRE', the 'ARTEMIS' ^{14}C AMS French Project and the ANR 'IDEGLACE'. We finally acknowledge A.M. McCabe, J.D. Scourse and Editor D.J.W. Piper for their helpful comments which greatly improved this paper. This is an UMR 5805 'EPOC' (Bordeaux 1 University — CNRS) contribution no. 1637.

References

Auffret, G., Zaragosi, S., Dennielou, B., Cortijo, E., Van Rooij, D., Grousset, F., Pujol, C., Eynaud, F., Siegert, M., 2002. Terrigenous fluxes at the Celtic margin during the last glacial cycle. Marine Geology 188 (1-2), 79–108.

Bard, E., 1998. Geochemical and geophysical implications of the radiocarbon calibration. Geochimica Cosmochimica Acta 62, 2025–2038.

Bard, E., Rostek, F., Turon, J.L., Gendreau, S., 2000. Hydrological impact of Heinrich events in the subtropical Northeast Atlantic. Science 289, 1321–1324.

Bond, G., Heinrich, H., Broecker, W., Labeyrie, L., McManus, J., Andrews, J., Huon, Jantschik, R., Clasen, S., Simet, C., Tedesco, K., Klas, M., Bonani, G., Ivy, S., 1992. Evidence for massive discharges of icebergs into the North Atlantic ocean during the last glacial period. Nature 360, 245–249.

Bond, G., Broecker, W., Johnsen, S., McManus, J., Labeyrie, L., Jouzel, J., Bonani, G., 1993. Correlations between climate records from North Atlantic sediments and Greenland ice. Nature 365, 143–147.

Boulton, G., Hagdorn, M., 2006. Glaciology of the British Isles Ice Sheet during the last glacial cycle: form, flow, streams and lobes. Quaternary Science Reviews 25 (23-24), 3359–3390.

Bouma, A.H., 1962. Sedimentology of Some Flysch Deposits: a Graphic Approach to Facies Interpretation. Elsevier, Amsterdam. 168 pp.

Bourillet, J.F., Turon, J.L., 2003. Rapport de mission MD133-SEDICAR. 150 pp.

Bourillet, J.F., Reynaud, J.Y., Baltzer, A., Zaragosi, S., 2003. The "Fleuve Manche": the submarine sedimentary features from the outer shelf to the deep-sea fans. Journal of Quaternary Science 18 (3-4), 261–282.

Bowen, D.Q., Rose, J., McCabe, A.M., Sutherland, D.G., 1986. Correlation of Quaternary glaciations in England, Ireland, Scotland and Wales. Quaternary Science Reviews 5, 299–340.

Bowen, D.Q., Phillips, F.M., McCabe, A.M., Knutz, P.C., Sykes, G.A., 2002. New data for the Last Glacial Maximum in Great Britain and Ireland. Quaternary Science Reviews 21 (1-3), 89–101.

Buoncristiani, J.F., Campy, M., 2004. Expansion and retreat of the Jura ice sheet (France) during the last glacial maximum. Sedimentary Geology 165, 253–264.

Chapman, M.R., Shackleton, N.J., Duplessy, J.C., 2000. Sea surface temperature variability during the last glacial–interglacial cycle: assessing the magnitude and pattern of climate change in the North Atlantic. Palaeogeography, Palaeoclimatology, Palaeoecology 157 (1-2), 1–25.

Chappell, J., 2002. Sea level changes forced ice breakouts in the Last Glacial cycle: new results from coral terraces. Quaternary Science Reviews 21 (10), 1229–1240.

Clark, P.U., McCabe, A.M., Mix, A.C., Weaver, A.J., 2004. Rapid sea level rise at 19,000 years ago and its global implications. Science 304, 1141–1144. doi:10.1126/science.1094449.

Clarke, G.K.C., Marshall, S.J., Hillaire-Marcel, C., Bilodeau, G., Veiga-Pires, C., 1999. A glaciological perspective on Heinrich events. In: Clark, P.U., Webb, R.S., Keigwin, L.D. (Eds.), Mechanisms of Global Climate Change at Millennial Time Scales. AGU Geophysical Monograph, vol. 112, pp. 243–262. Washington D.C.

Dahlgren, K.I.T., Vorren, T.O., 2003. Sedimentary environment and glacial history during the last 40 ka of the Voring continental margin, mid-Norway. Marine Geology 193, 93–127.

Dansgaard, W., Johnsen, S.J., Clausen, H.B., Dahl-Jengen, D., Gundestrup, N.S., Hammer, C.U., Hvidberg, C.S., Steffensen, J.P., Sveinbjörnsdottir, A.E., Jouzel, J., Bond, G., 1993. Evidence for general instability of past climate from 250-kyr ice-core record. Nature 364, 218–220.

Dowdeswell, J.A., O'Cofaigh, C., Taylor, J., Kenyon, N.H., Mienert, J., Wilken, M., 2002. On the architecture of high-latitude continental margins: the influence of ice-sheet and sea-ice processes in the Polar North Atlantic. 2002 In: Dowdeswell, J.A., O'Cofaigh, C. (Eds.), Glacier-Influenced Sedimentation on High-Latitude Continental Margins, 203. Geological Society, London, pp. 33–54. Special Publications.

Droz, L., Auffret, G.A., Savoye, B., Bourillet, J.F., 1999. L'éventail profond de la marge Celtique: stratigraphie et évolution sédimentaire. Comptes rendus de l'Academie des Sciences Paris 328, 173–180.

Elliot, M., Labeyrie, L., Dokken, T., Manthe, S., 2001. Coherent patterns of ice-rafted debris deposits in the Nordic regions during the last glacial (10–60 ka). Earth and Planetary Science Letters 194 (1-2), 151–163.

Elverhoi, A., Hooke, R.L., Solheim, A., 1998. Late Cenozoic erosion and sediment yield from the Svalbard–Barents Sea region: implications for the understanding of glacierized basins. Quaternary Sciences Reviews 17, 209–241.

Evans, D.J.A., O'Cofaigh, C., 2003. Depositional evidence for marginal oscillations of the Irish Sea ice stream in southeast Ireland during the last glaciation. Boreas 32, 76–101.

Everest, J.D., Bradwell, T., Fogwill, C.J., Kubik, P.W., 2006. Cosmogenic 10BE age constraints for the Wester Ross Readvance moraine: insights into British Ice-Sheet behaviour. Geografiska Annaler. Series A. Physical Geography 88 (1), 9–17.

Eyles, N., McCabe, A., 1989. The Late Devensian (<22,000 BP) Irish Sea Basin: the sedimentary record of a collapsed ice sheet margin. Quaternary Science Reviews 8 (4), 307–351.

Eynaud, F., 1999. Kystes de dinoflagellés et évolution paléoclimatique et paléohydrologique de l'Atlantique Nord au cours du dernier cycle climatique du Quaternaire. Thèse de doctorat, Université Bordeaux 1, 291.

Eynaud, F., Zaragosi, S., Scourse, J.D., Mojtahid, M., Bourillet, J.F., Hall, I.R., Penaud, A., Locascio, M., Reijonen, A., 2007. Deglacial laminated facies on the NW European continental margin: the hydrographic significance of British Ice sheet deglaciation and Fleuve Manche paleoriver discharges. Geochemistry, Geophysics, Geosystems 8 (1). doi:10.1029/2006GC001496.

Fairbanks, R.G., 1989. A 17,000-year glacioeustatic sea level record: influence of glacial melting on the Younger Dryas event and deep-ocean circulation. Nature 342, 637–642.

Forsström, P.L., Greve, R., 2004. Simulation of the Eurasian ice sheet dynamics during the last glaciation. Global and Planetary Change 42, 59–81.

Gilbert, R., Nielsen, N., Moller, H., Desloges, J.R., Rasch, M., 2002. Glacimarine sedimentation in Kangerdluk (Disko Fjord), West Greenland, in response to a surging glacier. Marine Geology 191 (1-2), 1–18.

Grousset, F.E., Pujol, C., Labeyrie, L., Auffret, G., Boelaert, A., 2000. Were the North Atlantic Heinrich events triggered by the behavior of the European ice sheets? Geology 28 (2), 123–126.

Hesse, R., Rashid, H., Khodabakhsh, S., 2004. Fine-grained sediment lofting from meltwater-generated turbidity currents during Heinrich events. Geology 32 (5), 449–452.

Hiemstra, J.F., Evans, D.J.A., Scourse, J.D., McCarroll, D., Furze, M. F.A., Rhodes, E., 2006. New evidence for a grounded Irish Sea glaciation of the Isles of Scilly, UK. Quaternary Science Reviews 25, 299–309.

Hinderer, M., 2001. Late Quaternary denudation of the Alps, valley and lake fillings and modern river loads. Geodinamica Acta 14, 231–263.

Hughen, K.A., et al., 2004. Marine04 Marine Radiocarbon Age Calibration, 0–26 cal kyr BP. Radiocarbon 46, 1059–1086.

Ivy-Ochs, S., Schäfer, J., Kubik, P.W., Synal, H.-A., Schlüchter, C., 2004. Timing of deglaciation on the northern Alpine foreland (Switzerland). Eclogae Geologicae Helvetiae 97 (1), 47–55.

Ivy-Ochs, S., Kerschner, H., Kubik, P.W., Schlüchter, C., 2006. Glacier response in the European Alps to Heinrich Event 1 cooling: the Gschnitz stadial. Journal of Quaternary Science 21 (2), 115–130.

Knies, J., Vogt, C., Matthiessen, J., Nam, S.I., Ottesen, D., Rise, L., Bargel, T., Eilertsen, R.S., 2007. Re-advance of the Fennoscandian Ice Sheet during Heinrich Event 1. Marine Geology 240 (1-4), 1–18.

Knutz, P.C., Hall, M.A., Zahn, R., Rasmussen, T.L., Kuijpers, A., Moros, M., Shackleton, N.J., 2002a. Multidecadal ocean variability and NW European ice sheet surges during the last deglaciation. Geochemistry, Geophysics, Geosystems 3 (12), 1077. doi:10.1029/2002GC000351.

Knutz, P.C., Jones, E.J.W., Austin, W.E.N., van Weering, T.C.E., 2002b. Glacimarine slope sedimentation, contourite drifts and bottom current pathways on the Barra Fan, UK North Atlantic margin. Marine Geology 188 (1-2), 129–146.

Knutz, P.C., Zahn, R., Hall, I.R., 2007. Centennial-scale variability if the British Ice Sheet: implications for climate forcing and Atlantic meridional overturning circulation during the last deglaciation. Paleoceanography 22. doi:10.1029/2006PA001298 PA1207.

Kucera, M., Rosell-Mele, A., Schneider, R., Waelbroeck, C., Weinelt, M., 2005. Multiproxy approach for the reconstruction of the glacial ocean surface (MARGO). Quaternary Science Reviews 24 (7-9), 813–819.

Lambeck, K., Yokoyama, Y., Purcell, T., 2002. Into and out of the Last Glacial Maximum: sea-level change during Oxygen Isotope Stages 3 and 2. Quaternary Science Reviews 21 (1-3), 343–360.

Larsonneur, C., Auffret, J.P., Smith, A.J., 1982. Carte des paléo-vallées et des bancs de la Manche orientale (1/50 000). BRGM, Brest.

Le Suavé, R., 2000. Synthèse bathymétrique et imagerie acoustique. zone économique exclusive (ZEE). Atlantique nord-Est, Brest, Editions IFREMER.

Lekens, W.A.H., Sejrup, H.P., Haflidason, H., Petersen, G.O., Hjelstuen, B., Knorr, G., 2005. Laminated sediments preceding Heinrich event 1 in the Northern North Sea and Southern Norwegian Sea: origin, processes and regional linkage. Marine Geology 216 (1-2), 27–50.

Lericolais, G., 1997. Evolution du Fleuve Manche depuis l'Oligocène: stratigraphie et géomorphologie d'une plate-forme continentale en régime périglaciaire. Thèse de doctorat, Université Bordeaux 1, 265 pp.

Mansor, S., 2004. Faciès sismique et architecture du système turbiditique armoricain. Rapport de Diplôme d'Etudes Approfondi. Université de Bretagne Occidentale. 51 pp. available online via the ASF website: http://www.sedimentologie.com.

Marks, L., 2002. Last Glacial Maximum in Poland. Quaternary Science Reviews 21 (1-3), 103–110.

McCabe, A.M., Clark, P.U., 1998. Ice-sheet variability around the North Atlantic Ocean during the last deglaciation. Nature 392, 373–376.

McCabe, A.M., Clark, P.U., Clark, J., 2005. AMS 14C dating of deglacial events in the Irish Sea Basin and other sectors of the British–Irish ice sheet. Quaternary Science Reviews 24 (14-15), 1673–1690.

McCabe, A.M., Clark, P.U., Clark, J., 2007a. Radiocarbon constraints on the history of the western Irish ice sheet prior to the Last Glacial Maximum. Geology 35 (2), 147–150.

McCabe, A.M., Clark, P.U., Clark, J., Dunlop, P., 2007b. Radiocarbon constraints on readvances of the British–Irish Ice Sheet in the northern Irish Sea Basin during the last deglaciation. Quaternary Science Reviews 26 (9-10), 1204–1211.

Ménot, G., Bard, E., Rostek, F., Weijers, J.W.H., E.C., H., Schouten, S., Sinninghe Damsté, J.S., 2006. Early reactivation of European Rivers during the last deglaciation. Science 313, 1623–1625.

Migeon, S., Weber, O., Faugères, J.-C., Saint-Paul, J., 1999. SCOPIX: a new X-ray imaging system for core analysis. Geo-Marine Letters 18, 251–255.

Mix, A.C., Bard, E., Schneider, R., 2001. Environmental processes of the ice age: land, oceans, glaciers (EPILOG). Quaternary Science Reviews 20, 627–657.

Mojtahid, M., Eynaud, F., Zaragosi, S., Scourse, J., Bourillet, J.F., Garlan, T., 2005. Palaeoclimatology and palaeohydrography of the glacial stages on Celtic and Armorican margins over the last 360 000 yrs. Marine Geology 224 (1-4), 57–82.

Naughton, F., Sanchez Goñi, M.F., Desprat, S., Turon, J.L., Duprat, J., Malaizé, B., Joli, C., Cortijo, E., Drago, T., Freitas, M.C., 2007. Present-day and past (last 25 000 years) marine pollen signal off western Iberia. Marine Micropaleontology 62 (2), 91–114.

Naughton, F., Sanchez Goñi, M.F., Turon, J.L., Duprat, J., Cortijo, E., Malaizé, B., Joli, C., Bard, E., Rostek, F., 2007. Wet to dry climatic trend in north western Iberia within Heinrich events. IX International Conference on Paleoceanography (ICP9), September 2007, Shanghai (China).

Nygard, A., Sejrup, H.P., Haflidason, H., Cecchi, M., Ottesen, D., 2004. Deglaciation history of the southwestern Fennoscandian Ice Sheet between 15 and 13 ^{14}C ka BP. Boreas 33, 1–17.

O'Cofaigh, C., Evans, D.J.A., 2007. Radiocarbon constraints on the age of the maximum advance of the British–Irish Ice Sheet in the Celtic Sea. Quaternary Science Reviews 26 (9-10), 1197–1203.

Peck, V.L., Hall, I.R., Zahn, R., Elderfield, H., Grousset, F., Hemming, S.R., Scourse, J.D., 2006. High resolution evidence for linkages between NW European ice sheet instability and Atlantic Meridional Overturning Circulation. Earth and Planetary Science Letters 243 (3-4), 476–488.

Peck, V.L., Hall, I.R., Zahn, R., Grousset, F., Hemming, S.R., Scourse, J.D., 2007. The relationship of Heinrich events and their European precursors over the past 60 ka BP: a multi-proxy ice-rafted debris provenance study in the North East Atlantic. Quaternary Science Reviews 26, 862–875.

Posamentier, H.W., Vail, P.R., 1988. Eustatic controls on clastic deposition II — Sequence and systems tract models. In: Wilgus, Ch.K., et al. (Ed.), Sea-level Changes: an Integrated Approach. Social and Economic Paleontological Mineral. Special Publication, 42, pp. 125–154.

Rashid, H., Hesse, R., Piper, D.J.W., 2003. Origin of unusually thick Heinrich layers in ice-proximal regions of the northwest Labrador Sea. Earth and Planetary Science Letters 208 (3-4), 319–336.

Reynaud, J.Y., Tessier, B., Proust, J.N., Dalrymple, R., Marsset, T., DeBatist, M., Bourillet, J.F., Lericolais, G., 1999. Eustatic and hydrodynamic controls on the architecture of a deep shelf sand bank (Celtic Sea). Sedimentology 46 (4), 703–721.

Rinterknecht, V.R., Clark, P.U., Raisbeck, G.M., Yiou, F., Bitinas, A., Brook, E.J., Marks, L., Zelcs, V., Lunkka, J.P., Pavlovskaya, I.E., Piotrowski, J.A., Raukas, A., 2006. The last deglaciation of the southeastern sector of the Scandinavian Ice Sheet. Science 311 (5766), 1449–1452.

Scourse, J.D., 1991. Late Pleistocene Stratigraphy and Palaeobotany of the Isles of Scilly. Philosophical Transactions of the Royal Society of London B334, pp. 405–448.

Scourse, J.D., Austin, W.E.N., Bateman, R.M., Catt, J.A., Evans, C.D. R., Robinson, J.E., Young, J.R., 1990. Sedimentology and micropaleontology of glacimarine sediments from the Central and Southwestern Celtic Sea. Special Publication of the Geological Society of London 53, 329–347.

Scourse, J.D., Furze, M.F.A., 2001. A critical review of the glaciomarine model for Irish sea deglaciation: evidence from

southern Britain, the Celtic shelf and adjacent continental slope. Journal of Quaternary Science 16 (5), 419–434.

Siddall, M., Rohling, E.J., Almogi-Labin, A., Hemleben, C., Meischner, D., Scheizmer, I., Smeed, D.A., 2003. Sea-level fluctuations during the last glacial cycle. Nature 423, 853–858.

Skene, K.I., Piper, D.J.W., 2003. Late Quaternary stratigraphy of Laurentian Fan: a record of events off the eastern Canadian continental margin during the last deglacial period. Quaternary International 99−100, 135–152.

Skinner, L.C., McCave, I.N., 2003. Analysis and modelling of gravity- and piston coring based on soil mechanics. Marine Geology 199 (1-2), 181–204.

Stow, D.A.V., Piper, D.J.W., 1984. Deep-water fine-grained sediments: facies model. Fine-grained sediments: deep-water processes and facies. Geological Society, Special Publication 15, 611–645.

Stow, D.A.V., Howell, D.G., Nelson, H.C., 1985. Sedimentary, Tectonic, and sea-level controls. In: Bouma, A.H., Normark, W.R., Barnes, N.E. (Eds.), Submarine Fans and related Turbidite Systems. Springer, New-York, pp. 15–22.

Stuiver, M., Reimer, P.J., 1993. Extended 14C data base and revised CALIB radiocarbon calibration program. Radiocarbon 35, 215–230.

Stuiver, M., Reimer, P.J., Reimer, R.W., 2005. CALIB 5.0. WWW program and documentation.

Turon, J.L., Bourillet, J.F., 2004. Rapport de mission MD141-ALIENOR. 45 pp.

Uehara, K., Scourse, J.D., Horsburgh, K.J., Lambeck, K., Purcell, A.P., 2006. Tidal evolution of the northwest European shelf seas from the Last Glacial Maximum to the present. Journal of Geophysical Research 111, C09025. doi:10.1029/2006JC003531.

Waelbroeck, C., Labeyrie, L., Michel, E., Duplessy, J.C., McManus, J.F., Lambeck, K., Balbon, E., Labracherie, M., 2002. Sea-level and deep-water temperature changes derived from benthic foraminifera isotopic records. Quaternary Science Reviews 21, 295–305.

Watts, W.A., 1980. Regional variation in the response of vegetation to Lateglacial climatic events in Europe. In: Lowe, J.J., Gray, J.M., Robinson, J.E. (Eds.), Studies in the Lateglacial of North West Europe. Pergamon Press, Oxford, pp. 1–22.

Weaver, P.P.E., Benetti, S., 2006. The North Atlantic deep-sea floor-glacial versus interglacial controls and comparisons between the eastern and western North Atlantic. Geophysical Research Abstracts 8, 10678.

Weaver, P.P.E., Wynn, R.B., Kenyon, N.H., Evans, J., 2000. Continental margin sedimentation, with special reference to the north-east Atlantic margin. Sedimentology 47 (1), 239–256.

Wilson, L.J., Austin, W.E.N., Jansen, E., 2002. The last British Ice Sheet: growth, maximum extent and deglaciation. Polar Research 21 (2), 243–250.

Yokoyama, Y., Lambeck, K., De Deckker, P., Johnston, P., Fifield, L.K., 2000. Timing of the Last Glacial Maximum from observed sea-level minima. Nature 406, 713–716.

Zaragosi, S., Auffret, G.A., Faugeres, J.C., Garlan, T., Pujol, C., Cortijo, E., 2000. Physiography and recent sediment distribution of the Celtic Deep-Sea Fan, Bay of Biscay. Marine Geology 169 (1-2), 207–237.

Zaragosi, Le, S., Bourillet, Auffret, Faugères, Pujol, Garlan, 2001a. The deep-sea Armorican depositional system (Bay of Biscay), a multiple source, ramp model. Geo-Marine Letters 20 (4), 219–232.

Zaragosi, S., Eynaud, F., Pujol, C., Auffret, G.A., Turon, J.L., Garlan, T., 2001b. Initiation of the European deglaciation as recorded in the northwestern Bay of Biscay slope environments (Meriadzek Terrace and Trevelyan Escarpment): a multi-proxy approach. Earth and Planetary Science Letters 188 (3-4), 493–507.

Zaragosi, S., Bourillet, J.F., Eynaud, F., Toucanne, S., Denhard, B., Van Toer, A., Lanfumey, V., 2006. The impact of the last European deglaciation on the deep-sea turbidite systems of the Celtic–Armorican margin (Bay of Biscay). Geo-Marine Letters V26 (6), 317–329.